Marie Skłodowska-Curie Innovative Training Networks (ITN-ETN)

5Gwireless

Innovative Architectures, Wireless Technologies and Tools for High Capacity and Sustainable 5G Ultra-Dense Cellular Networks

H2020 Grant Agreement number: 641985

5Gwireless

WP2 – mmWave Communications

D2.1: STATE-OF-THE-ART ASSESSMENT OF 5G MMWAVE COMMUNICATIONS

Contractual Date of Delivery:	31/12/2015
Actual Date of Delivery:	29/04/2016
Responsible Beneficiary:	SIR
Contributing Beneficiaries:	HWU, UPC, TTI
Security:	Public
Nature:	Document
Version:	1.0

This project has received funding from the European Union's Horizon 2020 research and innovation programme under grant agreement No *641985*.

Document Information

Version Date: 1.0

Total Number of Pages: 74

Authors

Name	Organization	Email
Yoann Corre	SIR	ycorre@siradel.com
Grégory Gougeon	SIR	ggougeon@siradel.com
Florian Letourneux	SIR	fletourneux@siradel.com
Vedaprabhu Basavarajappa	TTI	veda@ttinorte.es
Beatriz Bedia	TTI	bbedia@ttinorte.es
Yi Tan	HWU	yi.tan@hw.ac.uk
Josep Vidal	UPC	josep.vidal@upc.edu
Adrian Agustin	UPC	adrian.agustin@upc.edu

Document History

Revision	Date	Modification	Contact Person
v1.0	29 April 2016	Final version	Yoann Corre

Executive Summary

Main objective of the European **5Gwireless** project, which is part of the H2020 Marie Slodowska-Curie ITN (Innovative Training Networks) program resides in the training and involvement of young researchers in the elaboration of future mobile communication networks, focusing on innovative wireless technologies, heterogeneous network architectures, new topologies (including ultra-dense deployments), and appropriate tools. The present Document D2.1 is the first deliverable of Work-Package 2 (WP2) that is specifically devoted to the modeling of the millimeter-wave (mmWave) propagation channels, and development of appropriate mmWave beamforming and signal processing techniques. Deliverable D2.1 gives a state-of-the-art on the mmWave channel measurement, characterization and modeling; existing antenna array technologies, channel estimation and precoding algorithms; proposed deployment and networking techniques; some performance studies; as well as a review on the evaluation and analysis tools.

D2.1 is divided in four main chapters, covering 1) the mmWave propagation channel characterization and modeling, 2) the beamforming techniques, 3) the signal processing algorithms, and 4) some networking aspects.

The global spectrum shortage faced by the wireless communication carriers has driven the investigation of mmWave technologies and deployments for next generation cellular known as 5G and IMT-2020 (International Mobile Telecommunication 2020). MmWave spectrum offers abundant and contiguous resources. Analysis and modelling of the wireless propagation channel are required to address the related new scenarios. Some of the key mmWave outdoor propagation characteristics are: a high level of attenuation due to vegetation, atmospheric gases, a high blockage loss due to buildings, human body and other obstacles typically found in urban environments, dominant contributions from reflections in Non-Line-Of-sight (NLOS) links, and a multi-path channel dispersion limited to only a few contributions. Strong rain attenuation is also a well-known factor that limits the propagation range of point-to-point backhaul links; however they do not play a significant role in the short-range radio links considered for 5G network densification. Channel models are necessary tools for the propagation characterization, but also for the design and evaluation of new mmWave technologies and systems, e.g. 3D beamforming or multi-user MIMO (Multi-Inputs Multi-Outputs). Therefore, some measurement studies have recently been conducted in outdoor urban environments, using channel sounder techniques combined with high-gain directive antennas and spatial scanning. The measured channel properties are exploited to configure geometry-based stochastic models, but also to verify the precision of ray-tracing deterministic models.

One of the main challenges in mmWave communications consists in compensating the strong propagation attenuation by high antenna gains. This can be achieved with aligned horn antennas on fixed point-to-point links. But mobile communications need for continuous adaptation; therefore directional beamforming based on large antenna arrays is required. D2.1 provides a broad overview and survey of the antenna array techniques and mmWave beamforming to date. Remark that the high considered frequencies allow for large antenna arrays or beamformers in a small form factor.

At conventional microwave frequencies, the design of the antennas and of the beamformer is decoupled in order to exploit the flexibility of full digital beamforming. This is no longer possible at mmWave as full digital signal processing is too expensive and leads to high power dissipations. To address this in 5G networks, new antennas must be designed where analogue beamforming is tightly coupled with digital precoding to achieve high gains at low complexity and cost.

The current state-of-the art in terms of signal processing required for analog beamforming and hybrid analog-precoding at mmWave is reviewed. In terms of analog beamforming the typical schemes are based on phase shifters or continuous aperture phased MIMO. On the other hand, the hybrid analog-digital systems rely on spatially sparse-based, codebook-based and CAP-MIMO based precoding. Additionally, low-precision ADCs with low-power consumption impacts on the total system design elucidating a trade-off between the achievable rate and energy consumption as a function of the number of bits of ADC.

The other topic where signal processing plays an important role is for the channel estimation. There are two approaches: *codebook beamtraining*, where a protocol for transmitting different codewords is used and the users do not estimate explicitly the channel, *and sparse channel estimation* where techniques based on compress sensing are considered for estimating the channel thanks to the sparsity properties of the mmWave channel.

Future 5G systems will rely on mmWave-based last mile network with ultra-dense node deployments, i.e. few meter Inter-Site Distance (ISD) indoors and between 50 m and 200 m outdoors. Ultra-dense networks introduce challenges related to the interference mitigation, heterogeneity management, and mobility management. To avoid frequent handover procedures, it is proposed to separate the control and data planes. The control channels would be provided by macro eNB operating in the microwave band, while high data rate services would be supported simultaneously by small-cells in the mmWave band. In addition, the communication protocols and access procedures will face difficulties due to the strong propagation losses: frequent outages and intermittent signal quality; new cell search and access procedures that are compliant with the high antenna directivity; channel sensing and feedback quantization adapted to the short channel coherence time; etc. Those new networking techniques are the object of active research investigations. Tools and methodologies that will be developed in the 5Gwireless project will contribute to their evaluation.

Table of Contents

List of Tables

List of Figures

List of Acronyms

Acronym	Definition
3GPP	3rd Generation Partnership Project
5G	5th Generation of mobile communication systems
ABG	Alpha-Beta-Gamma model
ADC	Analog to Digital Converter
AOA	Angle Of Arrival
AOD	Angle Of Departure
AR	Axial Ratio
ASE	Area Spectral Efficiency
BB	Baseband
BS	Base Station
CAP-MIMO	Continuous Aperture Phased MIMO
CI	Close-In reference model
CIF	Frequency-dependent CI model
CPW	Coplanar waveguide
CSCM	Correlation-Based stochastic channel model
CSI	Channel State Information
D2D	Device to Device
DLA	Discrete Lens Array
eNB	enhanced-Node B
ETSI	European Telecommunications and Standardisation Institute
ISD	Inter Site Distance
FDMA	Frequency Division Multiple Access
FIR	Finite Impulse Response
FMCW	Frequency-Modulated Continuous-Wave
FSF	Frequency Selective Fading
FSPL	Free Space Path-Loss
GAMP	Generalized Approximate Message Passing
GDP	Generalized Detection Probability
GT	Guard Time
GSCM	Geometry-based Stochastic Channel Model
IMT	International Mobile Telecommunication
ITN	International Training Networks
LNA	Low Noise Amplifier
LS MIMO	Large Scale MIMO parameters
LOS	Line Of Sight
LTE	Long Term Evolution
LTE-A	LTE-Advanced
MIMO	Multi Inputs Multi Outputs
MMSE	Minimum Mean Square Error
MmWave	Millimetre wave

MU-MIMO	Multi-user MIMO
MS	Mobile Station
NLOS	Non Line Of Sight
NYU	New York University
O2I	Outdoor to Indoor
O2O	Outdoor to Outdoor
OFDM	Orhtogonal Frequency Division Multiplexing
PA	Power Amplifier
PCB	Printed Circuit Board
PLE	Path-Loss Exponent
RACH	Random Access CHannel
RCP	RACH Cyclic Prefix
RF	Radio Frequency
Rx	Receiver
SC	Small-Cell
SE	Spectral Efficiency
SIW	Substrate Integrated Waveguide
SLL	Side Lobe Level
SNR	Signal to Noise Ratio
SU-MIMO	Single-user MIMO
TDD	Time Division Duplexing
TDMA	Time Division Multiple Access
TOA	Time Of Arrival
Tx	Transmitter
UE	User Element or User Equipment
UMa	Urban Macro
UMi	Urban Micro
V2V	Vehicle to Vehicle
VNA	Vector Network Analyser
WLAN	Wireless Large Area Network
WP	Work Package
XPD	Cross Polar Discrimination
XPR	Cross Polar Ratio

1. Introduction

5Gwireless aims at solving fundamental research challenges that encompass architectural, technological and modeling aspects of cellular networks design and analysis. They are grouped in three main categories: 1) Architectural Challenges (AC), referring to radical changes of architectures, topologies, protocols; 2) Technology Challenges (TC), referring to radical changes of transmission technologies; and 3) Methodological Challenges (MC), referring to radical changes to the modeling and analysis. This document is first deliverable in Work Package 2 (WP2): "mmWave communications", and aims at enhancing and assessing solutions that enable mmWave mobile access.

The extension of the wireless communication spectrum towards the millimetre waves (mmWave) is viewed as a key enabler for future high data rate and high capacity 5G mobile networks, in addition to ultra-dense networks and large MIMO antenna arrays. Several frequency bands are today candidates for access network deployments, including 28 GHz, 38 GHz, V-band (56 – 66 GHz) and E-band (71 - 76 GHz and 81 – 86 GHz), some being unlicensed or lightly licensed, with possible channel bandwidths of few hundreds of MHz or few GHz. MmWave is already widely employed in last-mile backhaul for line-of-sight point-to-point links, but also in recent Wireless LAN at 60 GHz (IEEE 802.11ad). Its advantage resides in the very wide available spectrum resource. The progress in technology (antennas, electronic components) and cost reduction makes large-scale system deployments a practical perspective.

WP2 investigations in the 5Gwireless project are devoted to advanced mmWave technologies and modelling, or more precisely:

- Measurement-based propagation channel characterization and statistical modelling;
- Enhancement and elaboration of deterministic propagation channel models;
- Investigation and prototyping on hybrid digital/analog beamforming antennas;
- New channel estimation and precoding techniques for hybrid systems;
- Assessment of future ultra-dense mmWave access networks.

Deliverable D2.1 gives a state-of-the-art on all investigated topics, with an overview on the scientific literature, technical challenges, solutions and perspective. It is organized as follows:

- Section 2 introduces mmWave propagation channel properties, in particular the strong path-loss and attenuations; the channel measurement techniques, stochastic modelling approaches and deterministic models are reviewed.
- As beamforming is mandatory to make possible the mobile mmWave communications, Section 3 describes the state-of-the-art in beamforming antennas and techniques.
- Section 4 presents the current innovations and research in signal processing; the channel estimation and antenna array precoding are adapted to the specificities of the mmWave propagation channel and mmWave beamforming antennas, and must enable multi-user MIMO (Multi-Inputs Multi-Outputs).

- Section 5 gives a short insight on the envisaged mmWave deployment strategies and required networking evolutions.
- Finally, section 6 gives a conclusion.

In each section 2-5, the technical challenges to be considered in the 5Gwireless project research are pointed out.

Note: according to its exact definition, the mmWave spectrum ranges from frequencies 30 GHz to 300 GHz; however mmWave is often referring to all frequencies between 10 GHz and 300 GHz investigated today for future 5G systems; this document is using this second definition, which is common and convenient.

2. MmWave propagation channel

For next generation 5G cellular system, small-cell access based on mmWave communication is one of the most promising technology candidates. The propagation properties are quite different from the one experienced in conventional cellular channels below 6GHz. A major impediment to mmWave communications, even at short range, is the high Path Loss (PL), attenuation due to foliage, and atmospheric absorption. In addition, the mmWave signals do not penetrate brick and concrete. Those means mmWave cells may have to be located strictly indoors or strictly outdoors, and emphasis on small cells with radii between 50–200 m.

Propagation loss characterization and modeling is required to elaborate appropriate network design topologies, antenna systems and asses the network coverage. Besides, the properties of the wideband propagation channel, i.e. delay spread, angle spread, Doppler, etc, affect the link performance and inter-link correlation. Realistic channel modeling is critical for designing and evaluating new multi-antenna mmWave technologies.

2.1. Main properties

The main characteristic of wave propagation at high frequencies is the strong path loss compared to sub-6GHz. Indeed, the antenna size of both transmitter and receiver needs to be adapted to the signal wave length which is in the order of few millimetres, making a small effective aperture to capture the transmitter energy. MmWave propagation has thus been first dedicated to indoor short-range transmission or wireless backhauling with the help of highly directive antennas with high gains compensating the path loss.
MmWave propagation is also affected by increasing atmospheric loss with frequency (Figure 1), with typical bands strongly attenuated [1]. The V-band for example, in the 60 GHz range, undergoes 16 dB/km attenuation while the E-band, in the 70-80GHz range, undergoes 0.5 dB/km. This shortens even more the 60 GHz propagation range, but it can be also an advantage for cell isolation thanks to low long-range interference [2].

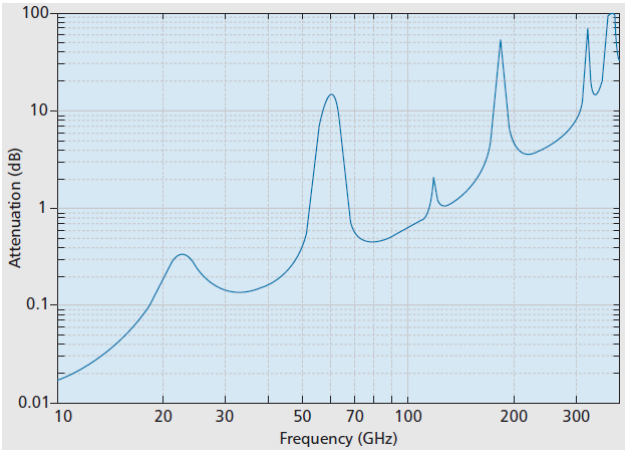

Figure 1. Atmospheric attenuation vs. operating frequency [1]

The impact of hydrometeors is also increasing with frequency and must be carefully taken into consideration when designing a link with high robustness requirement such as wireless backhaul. Figure 2 shows the attenuation occurring with various rainfall rates. If an attenuation of 8 dB/km may be negligible when considering a small-cell with 100 m radius, it will induce link failure (or capacity reduction) for longer range wireless backhaul. In order to limit such failure, statistical rain rates can be found in [3] (Figure 3) and used to define margin at the link design stage.

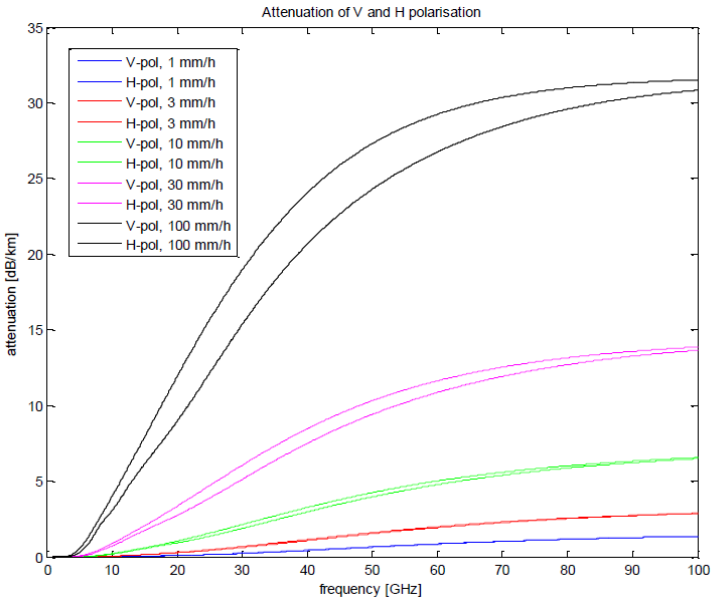

Figure 2. Hydrometeors attenuation vs. Operating frequency and rainfall rate [3]

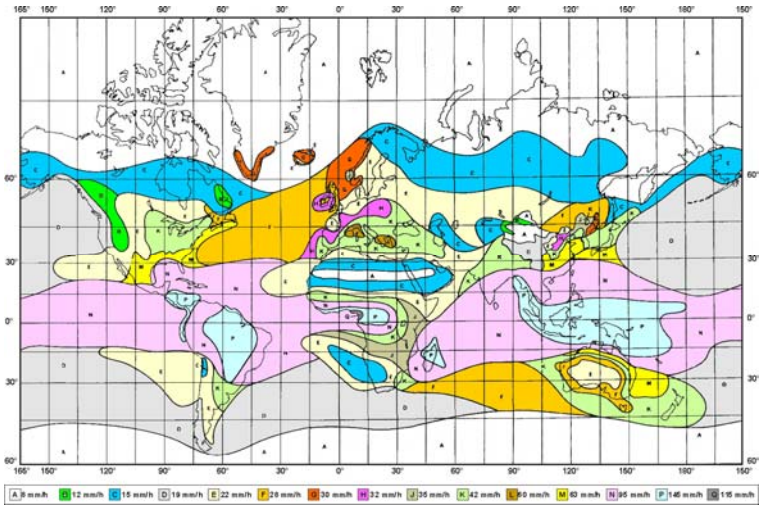

Figure 3. Map of the rain rate exceeded for 0.01% of the average year [3]

In Non Line-of-Sight (NLoS) condition, stronger attenuations affect the mmWave propagation compared to the sub-6GHz one. First, the transmission through walls is nearly inexistent. When considering the building material characteristics reported in Table 1 [4], the transmission through a concrete wall of 20 cm width leads to 21 dB attenuation at 6 GHz and 128 dB at 60 GHz (Figure 4). For a glass of 1.4 cm width, the transmission coefficient is 0.6 dB at 6 GHz and 8 dB at 60 GHz (Figure 5). Moreover, the modern windows often include metallic elements to increase the thermal isolation

performance; therefore attenuations up to 60 dB are possible.This concludes to an outdoor to indoor strong loss and with only the possibility of a penetration through windows, only if not coated with metal.

Table 1: Parameters for the relative permittivity and conductivity of building materials [4]

Material class	Relative permittivity	Conductivity		Frequency range (GHz)
		c	d	
Concrete	5.31	0.0326	0.8095	1-100
Brick	3.75	0.038	0.0	1-10
Plasterboard	2.94	0.0116	0.7076	1-100
Wood	1.99	0.0047	1.0718	0.001-100
Glass	6.27	0.0043	1.1925	0.1-100
Ceiling board	1.50	0.0005	1.1634	1-100
Chipboard	2.58	0.0217	0.7800	1-100
Floorboard	3.66	0.0044	1.3515	50-100
Metal	1	10^7	0.0	1-100

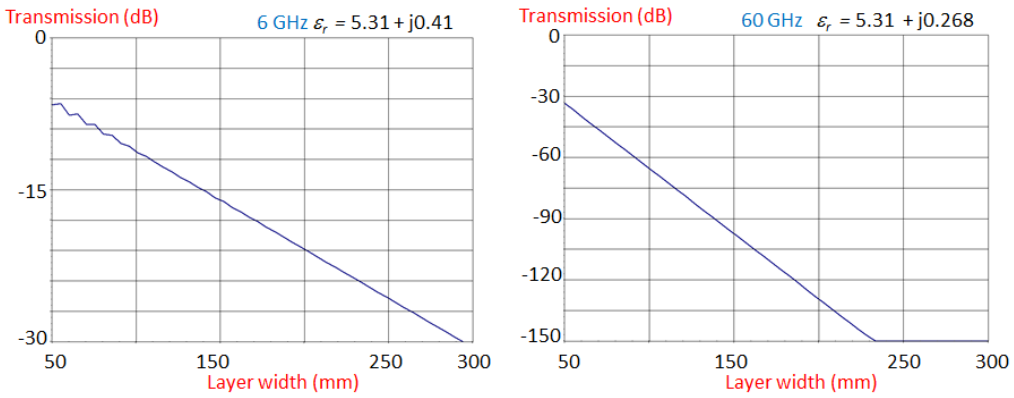

Figure 4: Transmission coefficient through concrete at 6 GHz (left) and 60 GHz (right)

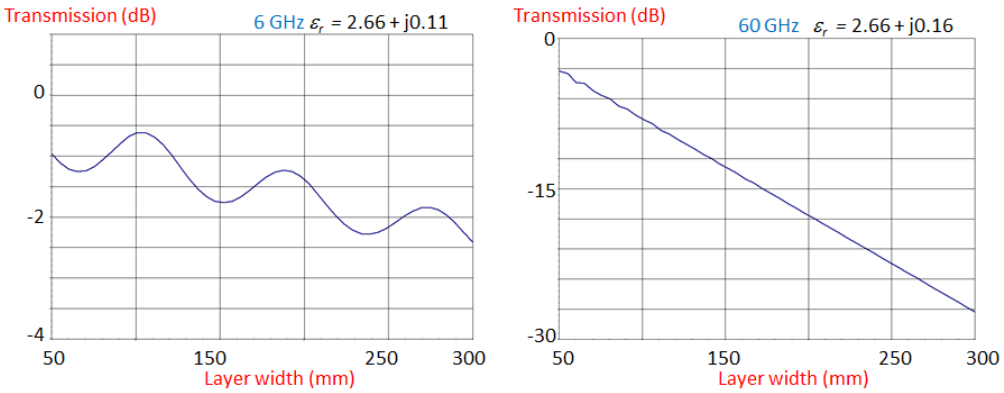

Figure 5. Transmission coefficient through glass at 6 GHz (left) and 60 GHz (right)

The diffraction loss is also more important at mmWave. The diffraction scenario illustrated in Figure 6 (left) is simulated considering the Knife-edge model based on the Fresnel integral [5]. The

diffraction coefficient is 10 dB higher at 60 GHz compared to the 6 GHz case. Actually, the mmWave channel does not exhibit rich multipath. It shows dominant paths coming from Line of Sight (LoS) direct path or strong reflections, and low diffused contributions [6]. Indeed, small details in the propagation environment being however larger than the wave length can lead to a strong reflectivity. The angular channel properties may be discarded due to high directive antennas, or exploited through MIMO processing like beamforming.

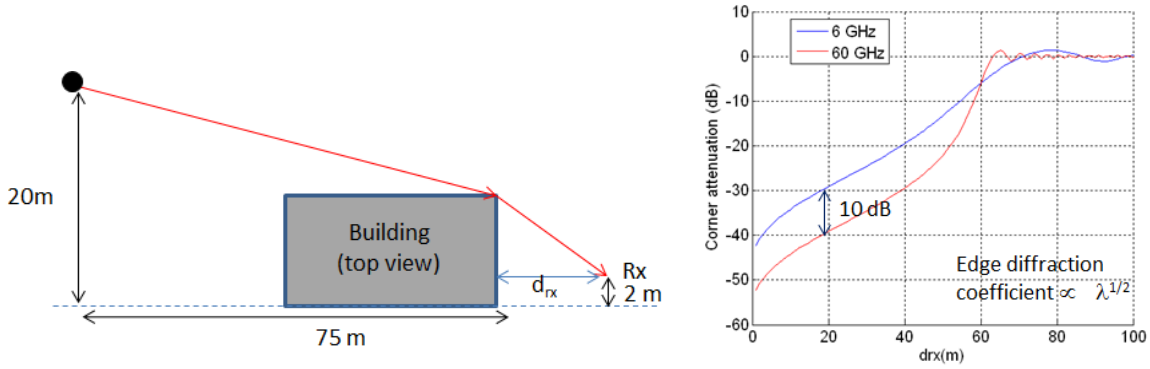

Figure 6. Diffraction scenario (left) and diffraction coefficient (right) at 6 and 60 GHz

Besides, the attenuation due to the vegetation is important. In [7], measurements at 57.6 GHz at two periods of the year showed an attenuation of 33 and 23 dB for one tree in the path, with and without leaves respectively. More important is the strong depolarization induced by the foliage. A cross polarization ratio of around 0 dB was observed on a path crossing 8 trees in leaf. In [8], measurements at 24 GHz showed a 2.6-3.8 dB/m attenuation in vegetation, or 20 dB per tree. The impact of foliage is moreover subject to high variability due to the wind. [9] indicates frequent drop-outs of up to 50 dB attenuation lasting for around 10 ms.

Finally, the human body shadowing has been characterized, showing strong attenuations up to 50 dB like in Figure 7 [10]. Intermittent link blockage can be alleviated thanks to beamforming as proposed in standards 802.11ad or 802.15.3c, in which the transmission can switch dynamically to another strong reflected path when the direct path is obstructed. In [11], 60 GHz measurements with and without human blockage shows for some location reflected paths with only a minor drop in signal power, relative to the LoS path.

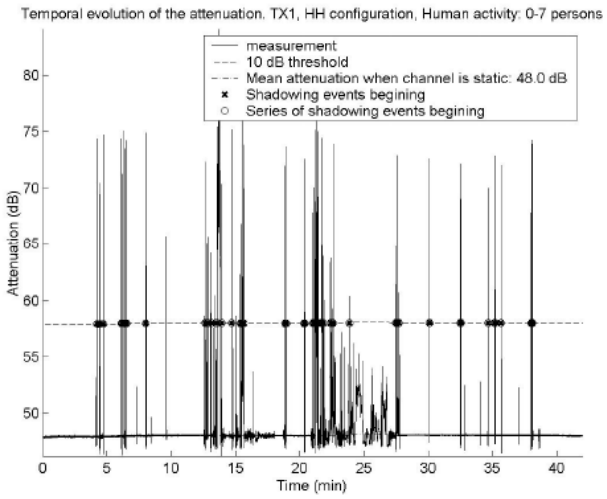

Figure 7. Temporal evolution of the attenuation at 60 GHz with 7 persons moving in a house and crossing the Tx-Rx link [10]

2.2. Measurement-based characterization

The future 5G communication systems arise the interests of the universities and the research institutes in North American, Europe, Asia and other parts of the world, the research about 5G channel models have been closely following this trend. The research results of mmWave channels published have been dramatically increased since 2012-2013. The channel measurements performed by NYU and Samsung in New York City have been considered as the ramp of the study of the mmWave channels [12]. The paper [12] gathers the results from four measurement campaigns at 28, 38, 60 and 73 GHz, from 2011 to 2013. The campaigns at 28 and 73 GHz carried out in NYU cover the Urban Micro (UMi) outdoor-to-outdoor (O2O) and outdoor-to-indoor (O2I) and Urban Macro (UMa) O2O scenarios, while the ones at 38 and 60 GHz in Austin cover the Urban macro O2O, Device-to-device (D2D) and vehicular scenarios, including vehicular-to-vehicular (V2V) and mobility in cellular deployment. The paper [12] summarizes the path-loss, spatial and temporal measurement-based results and subsequent models. The objective was also to offer a single reference and standard approach to allow the research community to share and compare results.

2.2.1. Path-loss, Shadow Fading and LoS probability

First, the channel is characterized by its optical visibility, i.e. the Rx being in LoS or NLoS of the Tx. The 3GPP and NYU LoS probabilistic models [13] [6] are tuned and evaluated in UMa and UMi scenarios in [14], showing similar behaviours. Note that the former was created using measured Rx locations, while the latter was generated using 3D map data and ray-tracing simulations.

Second, the path-loss is characterized and modelled by its path-loss exponent (PLE) and shadowing standard deviation. The paper [12] introduced above presents NYU path loss results at 28, 38 and 73 GHz. Directional path-loss results are directly extracted from data collected with rotatable directional horn antennas and are suitable for analysis of beamforming system path-loss. Then,

omni-directional results are synthesized from the raw data. The path-loss, Tx, Rx and map data information is given in [15] and forms to our knowledge the first mmW-band path-loss open dataset.

Close-in (CI) free space reference distance model and Alpha-Beta-Gamma (ABG) model, also called floating intercept, are proposed. In [16], both models as well as the CI model with a frequency-weighted path loss exponent (CIF) are calibrated and evaluated at various frequencies from 2 to 73 GHz and over distances up to about 1 km, from 30 measurement datasets. The model parameters, including PLE and the shadowing standard deviation are given in Table I, II, III and IV in the paper. The evaluation and sensitivity studies show that the physically-based CI and CIF models exhibit better overall accuracy and stability across frequencies and distances than the four-parameter ABG model [16]. In the CI model, there is an anchor point that ties path-loss to the Free-Space Path-Loss (FSPL) at 1 m, which captures the frequency-dependency and forms a uniform standard. In the CIF model there is one optimization parameter (n = PLE). In CIF, a second parameter (b) is added to tune the frequency dependency. Finally, in the ABG model, there are 3 parameters to calibrate the model and thus reduce the standard deviation.

These three omni-directional path-loss models are considered in different standardization bodies for 5G wireless simulation. The CI and CIF models can be implemented in existing 3GPP models by replacing the floating-based constant with a frequency-dependent constant.

Besides, [16] presents sets of parameters for the three omni-directional models for different propagation environments. The frequency range application is said to be 0.5-100 GHz. The very recent literature review in [17] lists PLE and shadow fading values from main characterization results published from 2011 to 2016.

PLE in outdoor UMa and UMi scenarios are not very frequency dependent [12], [16]. In LoS, path-loss is close to the theoretical FSPL (n = 2), while in NLoS most PLE range from 3 to 4 [17]. [14] proposes shadowing standard deviation values of about 4 and 7 dB, in respectively LoS and NLoS. However, [17] shows a significant variability in NLoS with values as high as 15 dB. Dependence of PLE and shadowing standard deviation on the base station and mobile antenna heights is not significant [17].

Third, for O2I scenarios, the building penetration loss and possibly indoor loss add up to the outdoor path-loss. The article [14] gathers some recent measurement results of single material and effective penetration losses including [18] and [19]. Overall, loss increases when frequency rises. Coated glass typically used in new buildings and renovations generates penetration loss as high as 40 dB. Paper [14] proposes two composite penetration building loss models, namely low loss and high loss models. The material loss is assumed to be proportional to the frequency. For instance, the building penetration losses at 40 GHz are 15 and 37 dB respectively. Moreover, [17] introduces a single penetration loss model (26.4 dB at 40 GHz) and a frequency-dependent shadowing model for UMi O2I scenario with shadowing standard deviation ranging from 8 to 10 dB. Finally, antennas located deeper into the building will suffer additional loss due to propagation and shadowing between external walls and them. It is mentioned in [14] a linear loss ranging from 0.2 to 2 dB/m and suggest to keep using the 3GPP value of 0.5 dB [13] for consistency purpose.

The blockage loss due to the obstruction by human bodies is a major issue, as introduced in the previous section. Many measurements on this topic have been published for indoor environments. But much less results are available outside. [11] recently presented a characterization of the human body blockage from LoS measurements conducted in a campus. Using a directive and steerable beam at the transmitter, the impact of human obstruction loss on the direct link (the blocker is placed in close vicinity of the receiver) can be evaluated, but also the capability of a reflected path (captured in another direction) to offer a relevant alternative during the blockage.

The blockage by the vegetation is another important property of the mmWave outdoor propagation, which contributes to make it very different than sub-6GHz propagation. The ITU recommendations in [9] reports an average linear loss of 0.2 dB/m at 1 GHz and 6 dB/m at 30 GHz, and proposes a methodology to estimate the attenuation through a woodland or isolated trees in the range from 300 MHz to 60 GHz. Besides, [8] investigates the propagation through vegetation at frequency 24 GHz based on directional vertically-polarized measurements, with rotation in both azimuth and elevation planes, and conducted in a campus with high vegetation density. Vegetation attenuation is found to be in the range 2.6 – 3.8 dB/m, at least for short vegetation propagation distances, while the attenuation by a single tree is estimated to be about 20 dB. The power level of some multi-paths scattered from the trees seem to be of similar order of magnitude as the power of building-reflected contributions.

2.2.2. Wideband channel properties

There is today a large effort in the scientific community, either in university laboratories or by equipment manufacturers, to elaborate measurement protocols devoted to mmWave channel sounding and collect samples in indoor and outdoor small-cell environments. The characterization of the 60 GHz indoor channel was already a concern about 15 years ago [20] with initial research on mmWave WLAN systems. As being a promising key enabler in 5G, the measurement-based characterization of the mmWave channel characteristics, i.e. measurement, analysis and modelling of the power delay profile, angular spreads, Doppler and multi-path depolarization, is of a much higher interest since a few years.

The main challenge is to detect all propagation directions along with the constraint to employ high-gain, and thus directive, antennas. We can basically distinguish between three different kinds of measurement systems to capture all those directions:

- Using highly-directive horn antennas at Tx or Rx side, or both, and scanning all directions at different successive times. This requires the measured channel to be constant during the whole measurement process. The process can take few tens of minutes or even hours if done manually. Synchronisation between Tx/Rx antennas is critical if it is fully automated. Furthermore, the overlapping between successive measured beams must be carefully taken into consideration when processing the measurements.
- Constructing a virtual antenna array, with challenges in terms of synchronization, location precision and calibration of the antennas.

- Using a multi-beam system that could provide real-time multi-direction measurements. To our knowledge, such system is not yet operational.

The wideband properties of the indoor channel have been measured and compared in three different frequency bands in [21], i.e. 2-4 GHz, 14 – 16 GHz and 28 – 30 GHz, showing that channel multi-paths is more sparse in mmWave bands (Figure 8), composed from only strong specular paths that can be easily identified with ray-tracing. The measurement system is composed of a VNA (Vector Network Analyser), a Tx omnidirectional antenna and a rotating Rx directive horn antenna that covers up to 720 different directions.

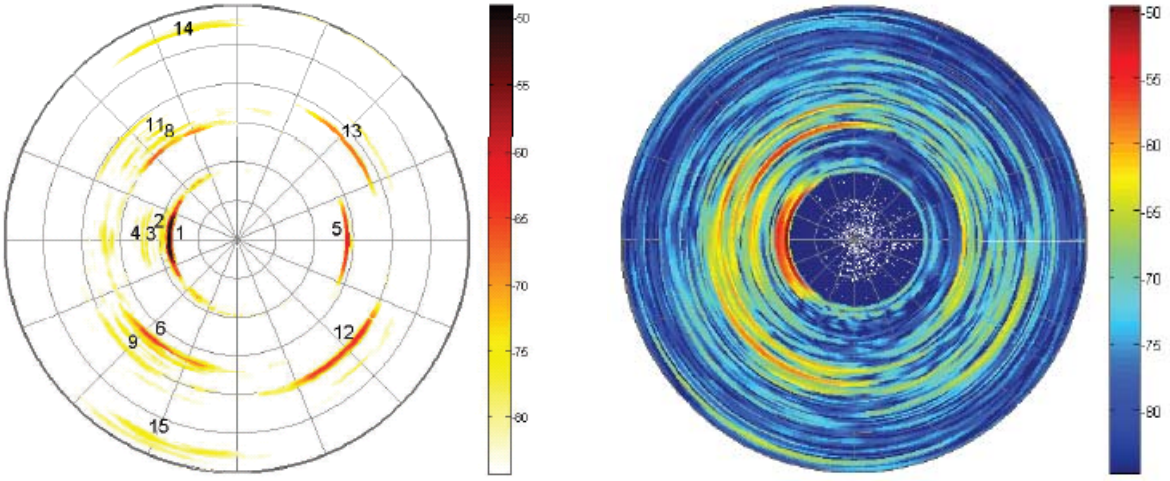

(a) Frequency band 14 - 16 GHz. (b) Frequency band 2 – 4 GHz.

Figure 8. Powerangledelayprofilemeasured at a LoSindoor link at twodifferentfrequencies [21]

A FMCW (Frequency Modulated Continuous Wave) channel sounder is employed in [22] to collect vertical-polarization power angle delay profiles at 60 GHz (with a rotating antenna) in both indoor and outdoor environments. The results show higher delay spreads indoors than outdoors: median RMS delays are respectively 4.7 ns and 13.7 ns at 60 GHz.

The outdoor channel dual-polarized measurements collected at 28 GHz and 73 GHz in New-York [23] are exploited to derive the parameters of 3GPP-like channel model in [24]. In particular, the NLOS angular spreads are found to be 22° and 6.2° at 28 GHz for respectively azimuth and elevation. The mean XPR (cross-polar ratio) is respectively 28.7 dB and 16.7 dB in LOS and NLOS at 28 GHz. About 5 clusters in average are identified in NLOS. An implementation of the proposed channel model has been made available as an open source since beginning of 2016.

Sub-millimeter frequency bands are nowadays meeting similar interest, still to find wider bandwidths for future 5G systems. For instance, [25] reports on measurements conducted in a small office in the two following frequency bands: 75 – 110 GHz, and 270 – 320 GHz. The channel sounder is formed by a VNA and two horn antennas and lenses installed on an automatically rotating platform. The sub-millimeter band exhibits highly specular power angle profiles that were made possible by the directive antennas (2° beamwidth) but also the specular nature of the channel itself.

2.3. Approaches for mmWave channel modelling

Since the technologies of wideband and MIMO are widely used in 2G/3G/4G telecommunication, the closely followed development of channel modelling methodologies according to the requirement of the telecommunication systems could be divided into 3 categories: 1) Stochastic channel model, 2) Deterministic channel model (measurement restoration or map-based model), 3) Hybrid channel model (combining stochastic and map-based models). See Figure Figure 9.

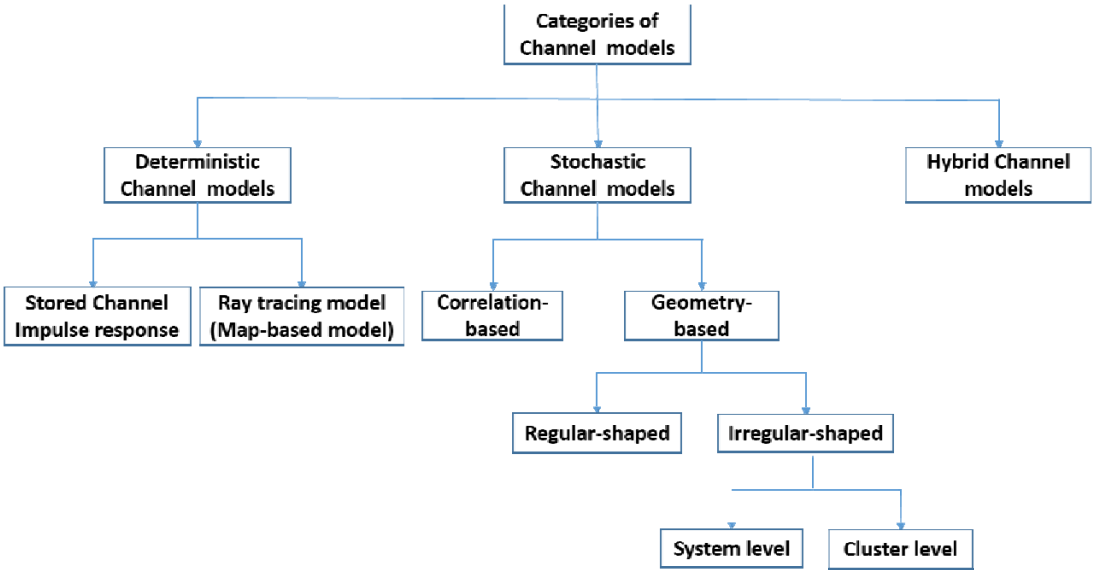

Figure 9. Categories of the channel models

Stochastic channel models could be generally divided into two categories: a) Correlation-Based stochastic channel model (CSCM), and b) Geometry-Based stochastic channel model (GSCM). The CSCM channel model describes the MIMO characteristics by correlation matrices; its merit is the lower computational complexity compared with the channel models in other categories; it is widely used by system level performance simulations. The well-known and widely used Kronecker model and Weichselberger model belong to this category. The difference between those two models is that, Kronecker model considers the Tx and Rx are not mutually correlated, but Weichselberger model could well present the joint correlation between Tx and Rx. The GSCM channel models are more accurate comparing with CSCM channel models, though it is with much higher computational complexity. It is a very important channel modelling approach that has been adopted in standards, and it is well accepted for mmWave domain.

For deterministic channel modelling, the typical solutions are a) the restored impulse response, and b) the ray tracing models. Restored impulse responses are acquired from channel measurements; it is the most direct way to present the wireless channel. Ray tracing is a site-specific approach that uses the geographical and morphological information of the certain wireless scenario for a deterministic application of a Maxwell's equation asymptotic approximation (construction of optical rays combined with Fresnel coefficients and the uniform theory of diffraction). In such way, it acquires the impulse response of the channel and the channel properties. The drawback is that it

requires large computational effort and the results are inherently less accurate. The main advantage is that computer simulations are easier to perform than measurement campaigns.

For mmWave channel modelling, stochastic channel model (more specifically GSCM), and Map-based (ray tracing) channel models are both well accepted. For example, NYU have derived a measurement-based stochastic model, and have been published some papers based on ray tracing models [26]. Furthermore, METIS mmWave Hybrid model [27] and IEEE802.11ad models combine the GSCM and ray tracing technologies together to provide a flexible and scalable channel modelling framework.

Other mmWave channel models, such as IEEE802.15.3c or mmMAGIC, are also available for study and system level performance simulation purpose.

2.3.1. Stochastic channel modelling

For the purpose of fast system-level simulations, stochastic channel models have been developed and standardized, and these are in constant evolution to deal with new systems and new topologies (Figure 10). This kind of models relies on statistical observations of the channel with various measurements in different typical environments. The distribution of various channel characteristics are extracted, then random realizations feed the system-level simulation and allow getting further statistics on the system performance.

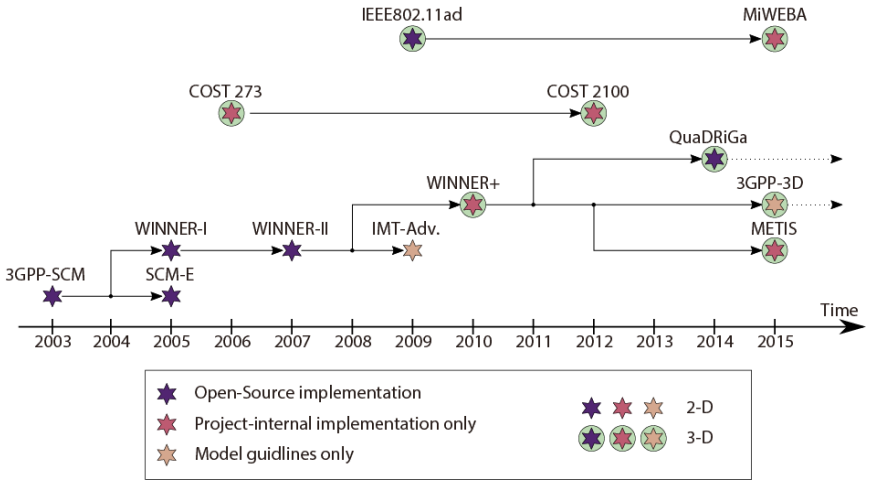

Figure 10. Channel models for cellular networks and their family history [17]

The concept of cluster has been early introduced: multi-paths can be gathered with similar propagation properties, firstly in the temporal dimension like in [28], then in the horizontal spatial dimension [29] [30] (Figure 11) and more recently in the vertical spatial dimension [13] [31], leading to 3D channel models. Indeed, multi-antenna systems require the knowledge of the direction of propagation of the multipath for relevant MIMO simulations.

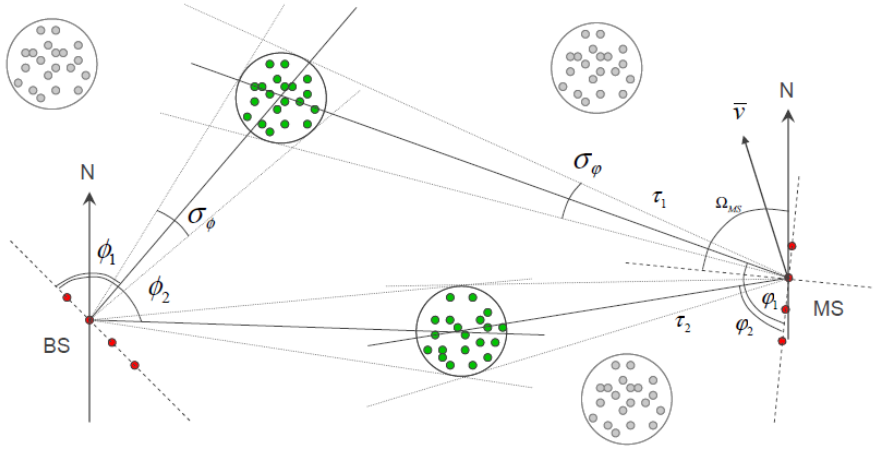

Figure 11. Cluster definition in WINNER II channel model [28]

Most of the stochastic models are Geometry-Based Stochastic Channel Models (GSCM). They can be divided into two categories: 1) Regular-shaped GSCM (pure-GSCM), and 2) Irregular-shaped GSCM (semi-GSCM). The Regular-shaped GSCM assume that the position of the scatterers and the clusters are distributed along a certain shape such as ring, ellipse, etc., with certain density function [32-36]. For irregular-shaped GSCM, the position of scatterers and clusters are not trackable; their spatial distribution obeys statistical distribution functions, such as those described in WINNER II or COST2100 channel models. They are further divided in two branches: 2.1) System-level approach, and 2.2) cluster-level approach [8].

The system-level approach, like in WINNER II, means that the statistics on the Large Scale Parameters (LSP) such as delay spread, angular spreads, shadow fading and K-factor are always guaranteed in each series of channel instances. The LSP are cross-correlated and remain constant along a predefined correlation distance. For each link, the clusters are randomly generated with respect to these LSP and remain valid over a short time. Each cluster gather several ray contributions (typically 20), which are assumed to be received by all the elements of the antenna array under plane wave assumption. To ensure continuity over a longer time, a birth-death process is proposed in [30].

It is also possible to define physical locations (x,y,z coordinates) of the clusters and their inner scatterers such that spherical wave assumption is respected for large antenna arrays [27]. In the cluster-level approach, for example the COST family models, the environment is described independently of the mobile station location. It is composed of clusters and their inner scatterers randomly located in space. This allows the spherical wave assumption to be respected for large antenna arrays [27]. Smooth modeling of time-variant channels is obtained thanks to visibility regions associated to the clusters. Naturally, in any single realization of the channel, a cluster-level GSCM is expected to exhibit larger deviations of the LSP statistics than system-level GSCMs.

Because stochastic channel models are based on measurements, these are limited to few scenarios and a frequency that is mostly below 6 GHz. Even if the model structure is still valid for mmWave, getting appropriate parameters requires challenging 3D channel sounding. Some new measurements provided parameters at 60 GHz for three WINNER 2 scenarios (shopping mall, cafeteria and outdoor open square). Recent European projects have addressed the issue. In the METIS project [27], some measurements have been done outdoors at 26 GHz (path loss only), and indoors at 58.7 GHz (path

loss, wall and body attenuation) and 63 GHz (channel sounding). Outdoor 3D channel sounding at mmWave is still insufficient to derive the model parameters.

2.3.2. Deterministic channel modelling

The ray-based models are already recognized as reliable tools to simulate accurate mmWave channel properties [12], [35], thanks to their ability to predict the dominant channel components, even in complex environments, and with reasonable computer resources. Ray-based models estimate the received power and channel properties (power delay profile, angles of departure, angles of arrival) from a geometrical optics approach. Specular reflections and diffractions are constructed from a detailed description of the environment. Diffuse scattering by large surfaces and scattering from small objects can also be integrated in such model, as soon as the scattered field can be expressed as a function of incident and scattered distances. The ray-based models are used to complement time-consuming and expensive measurement campaigns and to investigate mmWave propagation, coverage and system performance [38]-[40]. Furthermore, they are leveraged to parameterize and validate stochastic models [41]-[44].

Besides, the application of several antenna beams (from switching between different directive beams or from beamforming) is straightforward with ray-based model prediction outcomes, as the multiple propagation paths are characterized by their field and a discrete geometry.

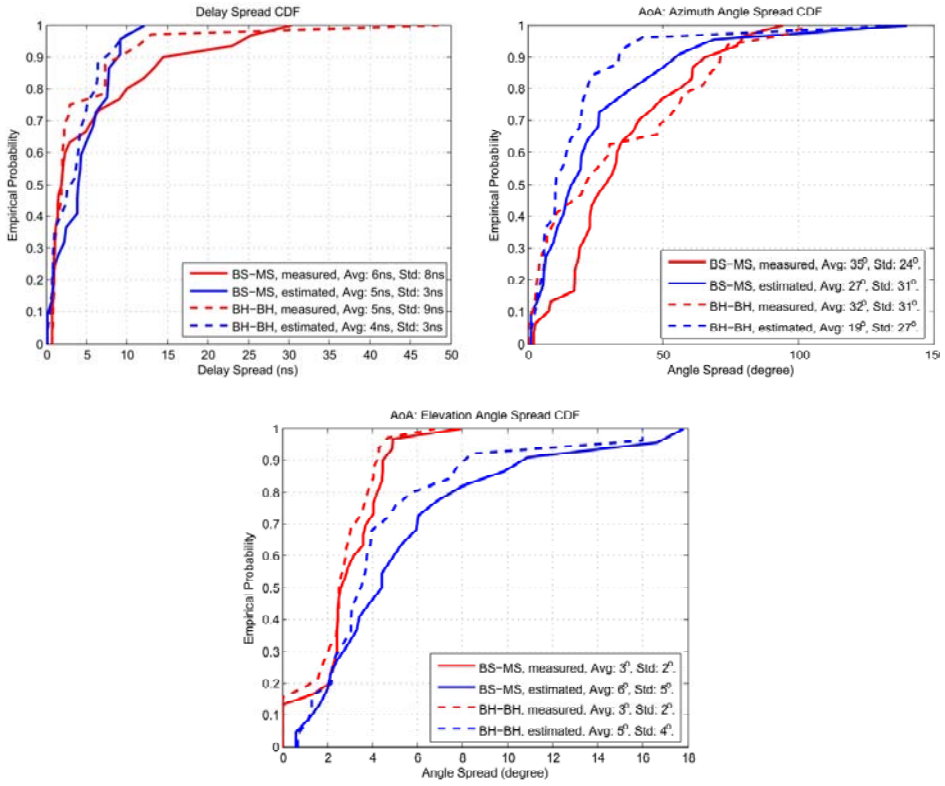

Figure 12. Comparisonbetweenmeasured and estimatedwideband cannel properties [34]

The relative importance of different propagation mechanisms that may be integrated in deterministic predictions (reflection, diffraction, scattering) was assessed by [45-[46] at frequencies 2.4, 5.8 and 28.0 GHz, and in macro-cell situations.

The article [37] presents a comparison between 3D ray-tracing model estimates and a measurement campaign made in NYU's campus in an urban scenario at 73GHz. The evaluated model aims to fill the gaps caused by the limited number of samples on measurements campaigns and facilitate an eventual site planning. It relies on a quite simple ray-based approach, and uses an environment representation of medium quality created from Open Street Map. However this model succeeds in predicting the mmWave channel properties as shown in Figure 12.

An insightful analysis is carried out in [34] about coverage, path loss, path diversity and delay spreads in downtown Manhattan area, based on ray-tracing simulations. The simulations outcomes are compared to on-field measurements taken by NYU and Samsung Electronics, showing a good match on the path loss and cluster diversity. However, the estimated delay spreads are lower than measured values, which are assumed to be related to the absence of small objects scattering in the simulation.

The article [47] uses ray-tracing to compare the coverage of a same small-cell (SC) urban deployment at 5 GHz and 60 GHz. The SC are placed in the streets with an average inter-site distance of 120m. The outdoor DL radio coverage of this network is simulated assuming system and propagation parameters specific to respectively sub-6GHz and mmWave frequency bands. The sub-6GHz parameters are based on typical 5 GHz outdoor WiFi deployments and equipment performances, while the mmWave network is assumed to implement beamforming at the SC and operates over a large frequency band, i.e. 250 MHz [48]. The ray-based model from [49] is used. The main conclusion illustrated in Figure 13 is that a SC deployment providing a seamless coverage at 5 GHz (with 2 dB SNR threshold) leads to 11% coverage outage at 60 GHz (with 8.5 dB SNR threshold).

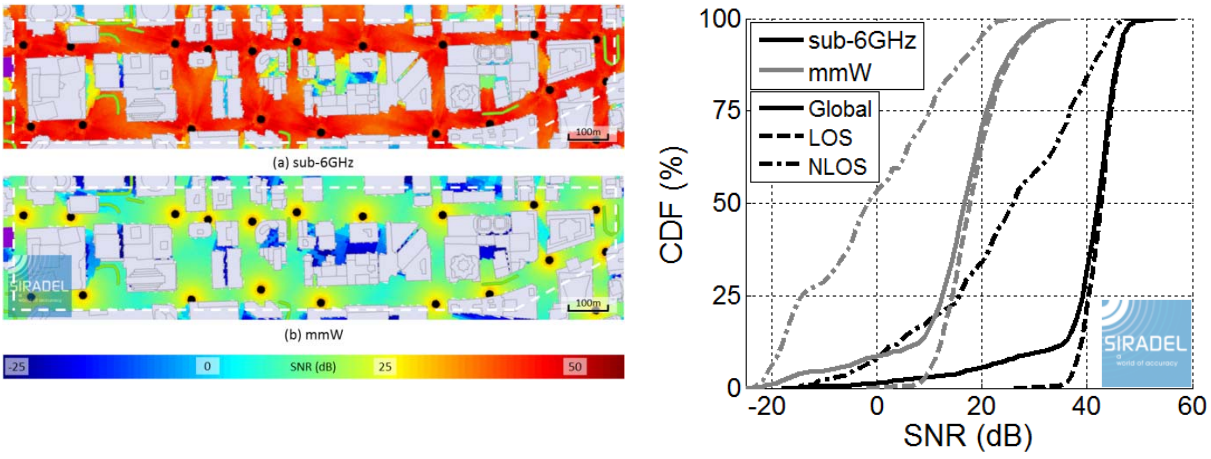

Figure 13. Comparison of small-Cell network coverage maps at 5 GHz and 60 GHz, based on the prediction of the Downlink signal-to-noise ratio (SNR) [47]

The same paper illustrates how the ray-tracing tools can complement the measurements to characterize the mmWave propagation channel. As shown in Figure 14, the impact of a complex

structure on the propagation loss, delay spread and angle spread is predicted at different frequencies. A small-cell and a user are separated by an individual house. Propagation and multiple scattering through the house are predominant at 2.4 GHz, while diffraction by the rooftop is the unique dominant path at 60 GHz. The results at 5 GHz show similar order of magnitude for both the propagation through the house and the propagation from rooftop diffraction.

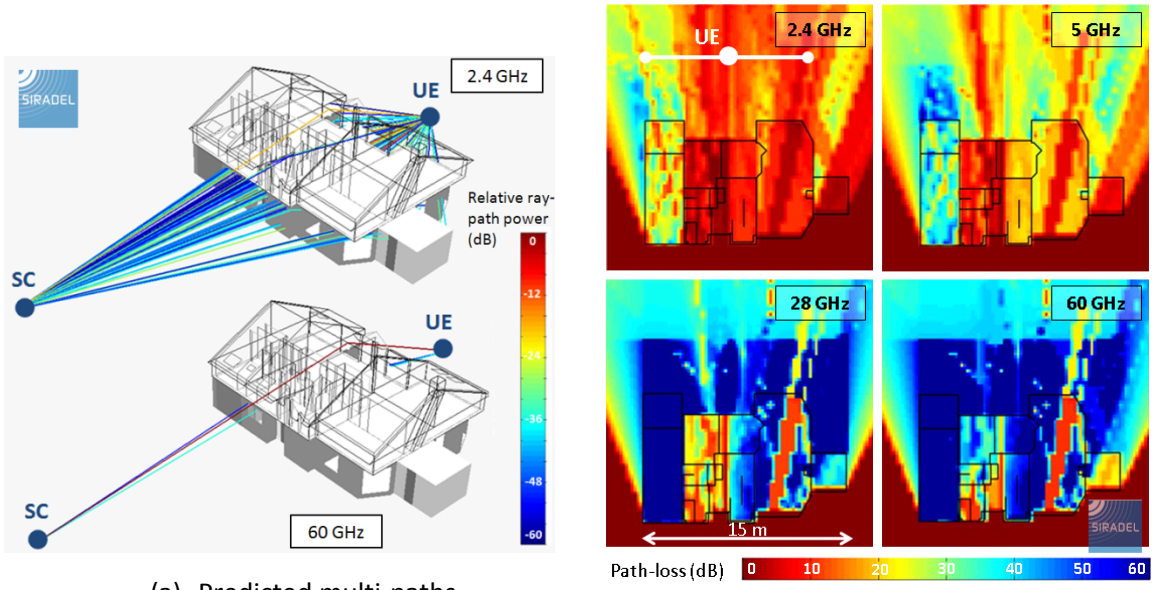

(a) Predicted multi-paths

(b) Predicted excess path-loss

Figure 14. Analysis of the propagation through a complex obstacle at 2.4 GHz and 60 GHz, from ray-based simulations [47]

2.3.1. Hybrid channel modelling

In hybrid model as proposed by METIS [27], the path-loss (PL) and shadowing are calculated from map, on top of that e.g. random shadowing objects can be generated. Then, all other calculations are performed by the stochastic model. To be able to use the hybrid model the locations of the BSs and the UEs have to be fixed on a map.

A hybrid modelling approach is emerging to address the mmWave, based on the representation of the channel impulse response as superposition of a few quasi-deterministic strong rays and a number of relatively weak random rays [50]. The mmMAGIC project plans also to extend the existing QuaDRiGa channel model with the help of deterministic simulations [17]. It must be noted that MiWEBA includes deterministic contributions in the simulation result while mmMAGIC uses the deterministic contributions to extract parameters for additional scenarios.

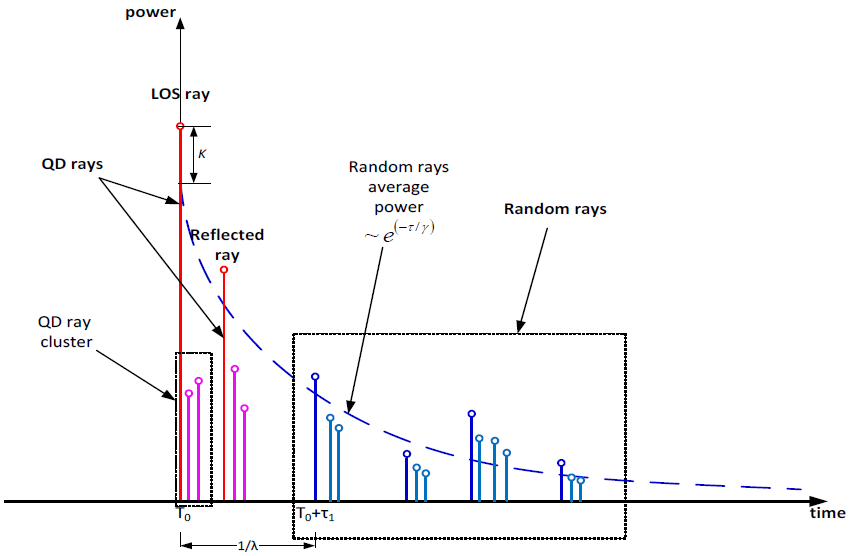

Figure 15. MiWEBA channel impulse response structure [50]

2.4. Tools for analysis of mmWave channels

2.4.1. MmWave channel sounder

Channel sounders are designed for channel measurements, and as the system design become more complex, the requirements of the channel sounding devices have evolved through three stages: 1) Be able to measure field strength in 1960s, 2) Be able to measure impulse responses – i.e., delay dispersion (wideband systems), 3) Be able to measure (Double) Directional impulse response since 1990s (multi-antenna systems/MIMO) [51]. The channel sounder used for measuring the directional channel impulse response have been inherited until today, with the extension to large antenna array (Massive MIMO) and the mmWave frequency, i.e. 5G wireless channels.

Generally, the channel sounders could be divided in to two types

1. Vector Network Analyzer (VNA) + antenna/antenna-array channel sounder,

2. Baseband components + RF components channel sounder, that is the typical RF signal transmission system, see Figure 16.

The former one measures the channel in frequency domain, and it could only measure the static channel scenarios, which are normally used for indoor scenarios. The later ones are mainly PN-sequence (correlative) sounders and OFDM signal transmission systems, which measure the wireless channel in time and frequency domains respectively. The advantage is that they could measure time-variant channels of both indoor and outdoor scenarios, such as V2V, M2M scenarios. More details could be found in the Chapter 8 of Molisch's book [51].

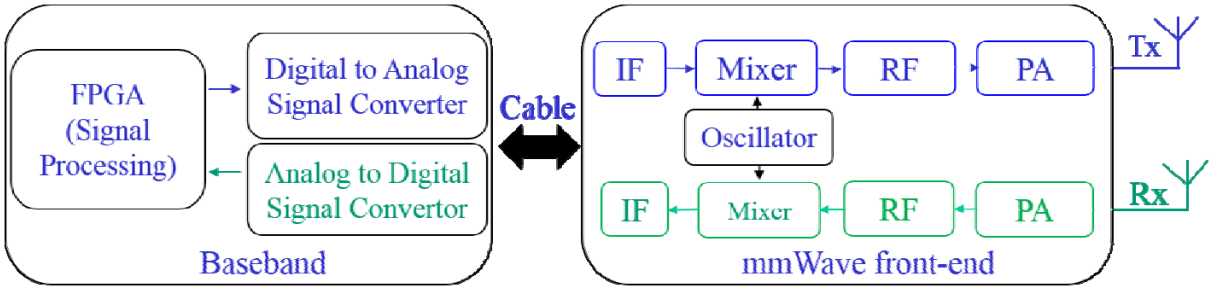

Figure 16. The typical structure of channel sounder

The channel sounders used in mmWave channel measurements also belong to above mentioned categories. Due to the cost, VNA + antenna-array channel sounder has been widely used by Universities and research institutes [52]. As the requirement of measuring time-variant mmWave channels, many universities and companies have started to develop the channel sounder based on baseband components + RF components, and more research results have been published based on such type of channel sounder. NYU [23], Technische Universität Ilmenau [53, 54], Fraunhofer Heinrich Hertz Institute [55], Electron. & Telecommun. Res. Inst (ETRI) South Korea [56], as well as the companies such as R&S, Keysight [57], Nutaq, etc. all have their mmWave channel sounder based on the baseband components + RF components setup. The Tx/Rx architecture of the NYU channel sounder at 28 GHz is illustrated in Figure 17 and Figure 18.

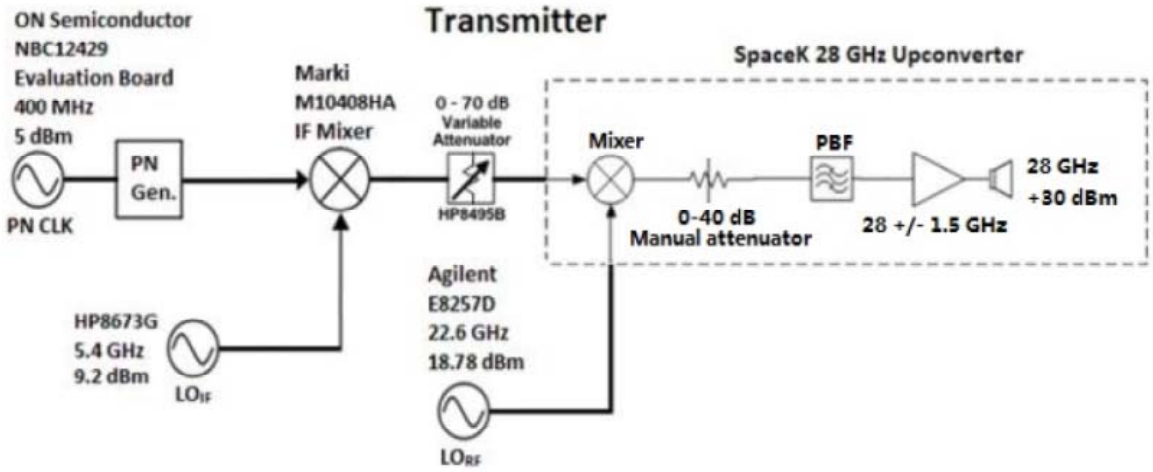

Figure 17. NYU channel sounder, Transmitter part

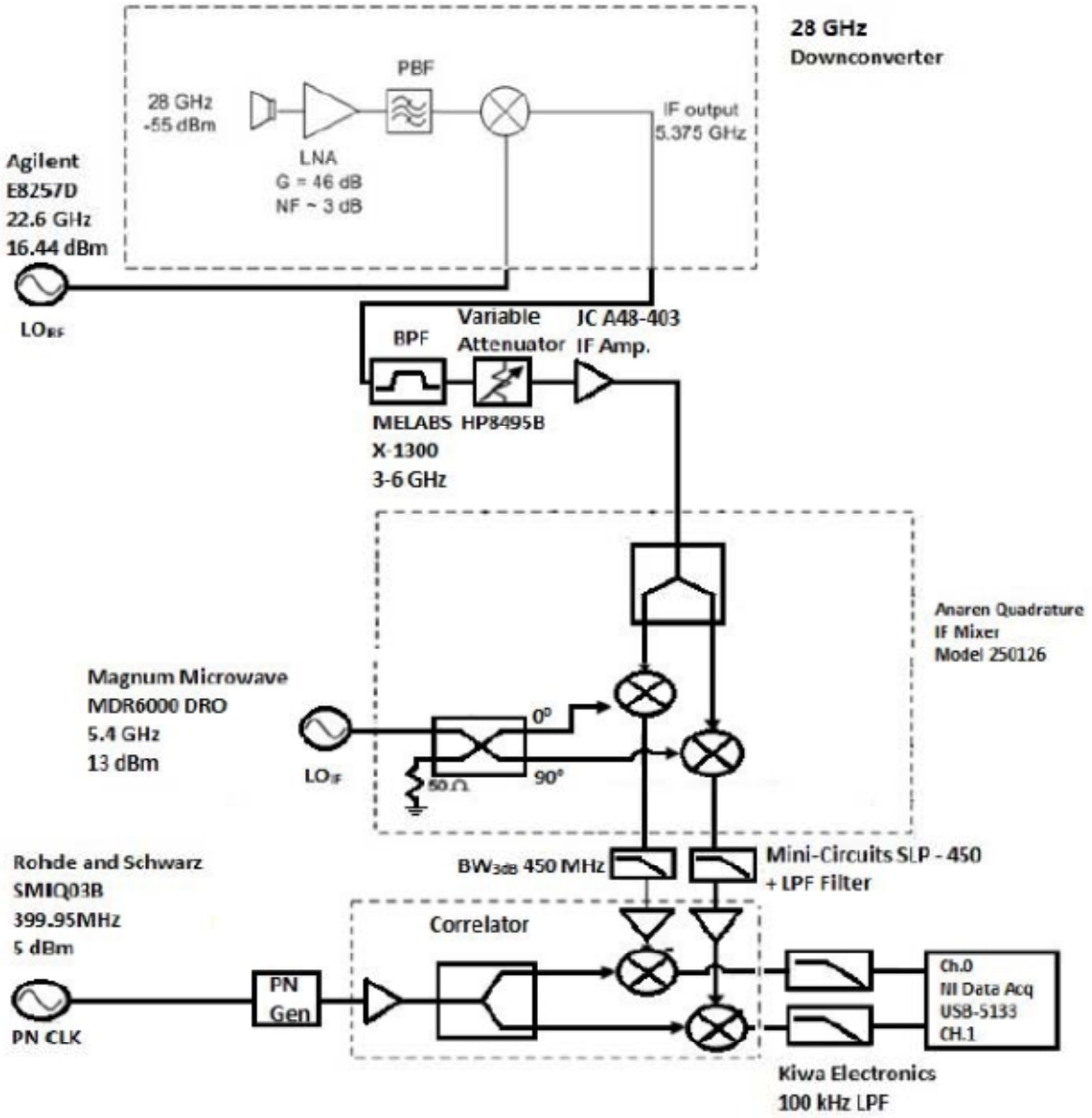

Figure 18. NYU channel sounder, Receiver part

2.4.2. Algorithms to calculate AoA, DoA, of the mmWave channel

The term of "channel" used here actually have been used in other areas as well, such as Acoustic Sensoring [59], GPS location, Optical and Seismology, etc., there are a lot of papers about detecting the angle of Arrival (AoA) using the algorithms such as Capon, MUSIC, ESPRIT, etc. before 1990s for example. It is very beneficial to the development of the channel estimation algorithms in wireless communication area, that since 1990s the measurement of the directional channel have been requested, those algorithms have been inherited directly and applied in the data processing of wireless channel measurements.

The algorithms used in directional channel estimation refer to time-delay estimation methods, and array signal processing, etc. The development of the channel estimation has been done in three stages:

1. Angle of arrival, due to narrow bandwidth sounding system at the beginning,

2. Joint angle and delay estimation (ToA + AoA), as the system bandwidth of channel sounder become broader and broader,

3. High-resolution angle and delay estimation. Since 3G and 4G, the algorithms of joint angle and delay estimation and high resolution algorithms are widely used, such as SAGE. And in the research about 5G channel, those high resolution algorithms are still suitable as well.

The algorithms used in joint angle and time estimation could be divided into three categories [60, 61]:

1. Covariance matrix based (subspace based) methods, such as JADE, ESPRIT, MUSIC,

2. Correlation-and-cancellation methods, such as CLEAN, which used in Ultra-WideBand (UWB) channels,

3. Maximum-likelihood parameter techniques, such as SAGE, which is widely used in mmWave channels.

Table 2. General DoA algorithm

General DoA methods			
	Conventional algorithms (Beamforming, MVM, MUSIC, JADE+MUSIC/ESPRIT, Unitary ESPRIT, etc.)	**CLEAN** (Correlation-and-cancellation)	**SAGE** (Maximum likelihood)
Prerequisite	Covariance matrix	Sum-and-delay beamforming	None
Implementation difficulty	Low	Middle	High
Resolution	Low	High	High
Speed of algorithms	Fast/Slow (singular value de-composition)	Slow	Slow
Data type (number of snapshots)	Multiple/One (Toeplitz covariance matrix)	One (generally)	One (generally)
Bandwidth	Narrow	Wide	Narrow/Wide
mmWave channel	Not in the publications	Not suitable (UWB bands)	Suitable

The proper algorithms need to be selected carefully, depending on the channel situation and the channel sounder system. Refer to Table 2. The covariance matrix based methods require the average of the estimation on many snapshots (the expectation operator), then they are suitable for the channel measurements done by correlative channel sounder (baseband + RF). For measuring indoor

environment with VNA + antenna-array channel sounder, the whole measurement only has one snapshot of the channel, therefore SAGE is a good choice in this case.

For the channel estimation requiring high resolution algorithms, SAGE is also very popular. To our knowledge, SAGE is very well accepted as the standard algorithm in data analysis of mmWave channels measurement. And no matter which type of channel sounder used in the measurement, SAGE is always a good choice in the data post-processing.

2.4.3. Simulation tools

Some public channel models have been accompanied with public Matlab code or other type of demo program, which should facilitate the simulation for the beginners. Many of those Matlab codes have been well written, with clear structure, such as Matlab code of WINNER II, IEEE802.11ad, and 3GPP SCM. Those examples could be found directly from devoted websites.

Matlab code and basic structure of later channel models can inherit and extend the former channel models code. It is very convenient when aligning a simulator with the state-of-art channel models. As an example, METIS standard channel models have extended the WINNER II models, with paramaters in the mmWave frequency range and up to 4GHz bandwidth.

Ray tracing software are other important tools that are widely used in mmWave channel simulation. For example, it has been introduced in IEEE802.11ad, IEEE802.15.3c and map-based METIS mmWave channel modelling. Many ray-tracing software exist, commercial, academic prototypes or open sources. First efficient and robust solutions emerged during the 90'ies first for the assessment of microcell or indoor power coverage, then for deterministic wideband channel characterization. The widely used commercial Ray tracing softwares that suitable for mmWave channels are: SIRADEL Volcano, Altair WinProp, Remcom Wireless Insite, etc.

2.5. Current leading researches of mmWave channel modelling.

The approaches of mmWave channel modeling mainly based stochastic channel models and ray tracing channel models. The research in this area is leading by Prof. Theodore (Ted) S. Rappaport in NYU [12, 15, 24, 26, 62-67] and the researchers in Samsung Electron., Co., Ltd. [68]. Many universities and companies that are also working on mmWave channel models. Some of them are: Lund University [52, 69], University of Texas [70], Electron. & Telecommun. Res. Inst (ETRI) South Korea [70, 72], Intel Corp. [36, 73-75], Huawei Technologies Co., Ltd. [76], HWU [77], etc.

European Commission has spent billions of Euros investigating the projects about future 5G communications based on the perspective of Horizon 2020. Among those projects, 5G Infrastructure Public Private Partnership (5G PPP) is taking the Europe's leadership in standardizing 5G communications, and have caught the attention from industry manufacturers, telecommunications operators, service providers, etc. As the 5GPP's litany of sub-groups, METIS-II and mmMAGIC projects have brought many universities and companies work together and committed to actively drive the collaboration with the 5G PPP, and the research of mmWave channel is one of the most

important areas in those projects. Until now, the METIS mmWave channel models [27] and the QuaDRiGa (mmMAGIC) mmWave channel models [17] are the best proposed models and the yields of the research results. Those mmWave channel models have provided us standardized references for the future study, and the open source Matlab coded they have shared are very valuable asset.

2.6. Research roadmap

The mmWave channel measurement and modelling are in a cross-verification relationship. The accuracy of the channel model need to be verified by the comparison with the real channel measurement. The channel measurement itself could be limited by the setup of the hardware and the circunstancies in the measurement, the reliability and repeatability is critical. The measurement results can be verified that it should not be very different from simulation result.

Due to the mmWave communication based on the frequency up to tens of GHz or even higher, and with very broad bandwidth, the mmWave channel properties are quite different from the former 3G/4G wireless channels. For example, the smaller objects in the channel scenario could be significantly effective to the property of the channel, and the WSSUS assumptions (stationarity) of the channel need to be verified. For stochastic channel modelling and the channel measurement, there are still a lot of work ahead. Here is a list of topics we are going to investigate in the 5G wireless project:

- Develop a novel general method to define the stationarity region for all the channel cases, which should be suitable for all time, frequency, and spatial domains.
- Investigate the stationarity pattern, find out which factors affect the stationarity region, such as the size of object, the antenna pattern, and the direction of the MPC, etc. Try to abstract the pattern as the condensed parameters.
- Do the investigation about the interrelation among stationarity in time, frequency and space, looking for trends, pattern and other factors that affect the interrelation.
- Propose a new mmWave model, which is based on the study of the stationarity of the channel in time, frequency and spatial domains. Insert the stationarity parameter in the procedure of creating the simulation models, those parameters could be considered as another limit to guarantee the simulation models does not violate the WSSUS (White Sense Stationary Uncorrelated Scattering) assumption.
- Perform the mmWave channel measurements in corresponding channel scenarios. The measurements could include various mmWave channel scenarios, which depend on the requirements of the research of the stationarity. The indoor mmWave channel measurement is a must.
- Verification of the newly developed mmWave channel models by the data analysis of the channel measurement. Keep improving the correctness and the accuracy of the model.
- Develop the test bed and user equipment (UE) for assessment and demo the performance of mmWave communication technologies. The program of signal transmission and reception parts in the channel sounder could be modified to meet this requirement, and both Tx and Rx of channel sounder should be fully duplex.

Although there is already some research where ray-tracing models are employed to characterize the mmWave channel properties, there is still a huge effort to be done before such models can be made appropriate and qualified in those challenging frequency bands. We list here below some of the key topics that would require additional research:

- Integration of small objects and any environment detail that generates significant propagation phenomena (shadowing and scattering):
    - Integration in the geographical map data (in a stochastic or deterministic way);
    - Integration in the channel simulation (in a stochastic or deterministic way);
- Modelling of the diffuse scattering coming from the building façades;
- Integration of the vegetation (from large vegetation blocks to isolated trees) in the environment and channel simulation;
- Integration of realistic space fading, in particular in presence of beamforming;
- Integration of time fading due to moving objects (human bodies and vehicles) in the propagation area;
- Prediction of O2I propagation mechanisms and signal levels;
- And overall, validation and error quantification, by comparing the simulations to a wider range of channel measurements, including co- and cross-polar components.

5G wireless will contribute in the research effort to make the ray-based models a reliable tool to predict the mmWave channel and assess the performance of mmWave techniques and network deployments.

3. Beamforming

3.1. Introduction

The recent increase in cellular traffic at the microwave frequency band has shifted the focus towards the underutilized wide mmWave spectrum. Current cellular networks, based on the postulate that high frequencies are unfavourable to cellular communications cannot keep pace with the mobile data explosion by maintaining the required spectral and energy efficiency. Cellular communications occur at microwave frequencies (below 3GHz). The postulate that higher frequencies (greater than 3 GHz) introduce a larger attenuation unfavourable to cellular communications cannot be relied upon. But at microwave frequencies the channel bandwidth is limited and since the area spectral efficiency (ASE in bits/Hz/m²) linearly increases (best-case) with bandwidth, the ASE would be limited; the spectral efficiency is as well bounded by the transmit power. 5G therefore cannot be designed on this postulate. Recently in 2013, experimental results showed that high frequencies are not that harmful for cellular communication. Experiments further showed that mmWave transmission is capable of offering an increased SE compared to lower frequency transmission. One of the challenges of this project involves overcoming unfavourable mmWave propagation by high gain beamforming antennas design. MmWave systems need to employ directional beamforming with very large antenna arrays at both transmitter and receiver in order to realize sufficient link margin to overcome the high path loss at high frequencies.

At conventional microwave frequencies, the design of the antennas and of the beamformer is decoupled in order to exploit the flexibility of full digital beamforming. This is no longer possible at mmWave as full digital signal processing is too expensive and leads to high power dissipations. To address this in 5G wireless project new antenna designs are proposed where analogue beamforming is tightly coupled with digital precoding to achieve high gains at low complexity and cost. A brief review of the mmWave beamforming and beamforming techniques in general and a state-of-the-art are discussed in next sections.

3.2. Key aspects on beamforming

Beamforming employs an array of antennas to radiate energy or capture it over its aperture in a particular direction. It can be considered as a spatial filtering operation. Smart antennas direct beams along desired directions and project nulls in undesired ones using beamforming. The challenges in contemporary telecommunication technology like the Massive MIMO demand that antennas are capable of scanning narrow beams, have low SLL (Side Lobe Level) and specially formed beams to mitigate interference. These further require the abilities of beamscanning and beamforming for mmWave antenna systems.
Phased arrays are one such technology that allows beamforming. The electronic beamsteering achieved in phased arrays is performed by exciting a particular array radiation pattern. The array radiation pattern is a product of the individual antenna element pattern and the array factor.

Adaptive beamforming involves knowing the direction of desired signal and undesired signals and then adaptively calculating the array excitation coefficients to point directional beam along the desired direction in space and nulls in the undesired direction. It is often referred to as spatial

filtering. An example for a simple array system consisting of four sensors with two impinging signals is shown in Figure 19 for illustrative purposes [78] where the direction of arrival (DOA) of the signals is characterized by two parameters: an elevation angleΘ and an azimuth angle ϕ.

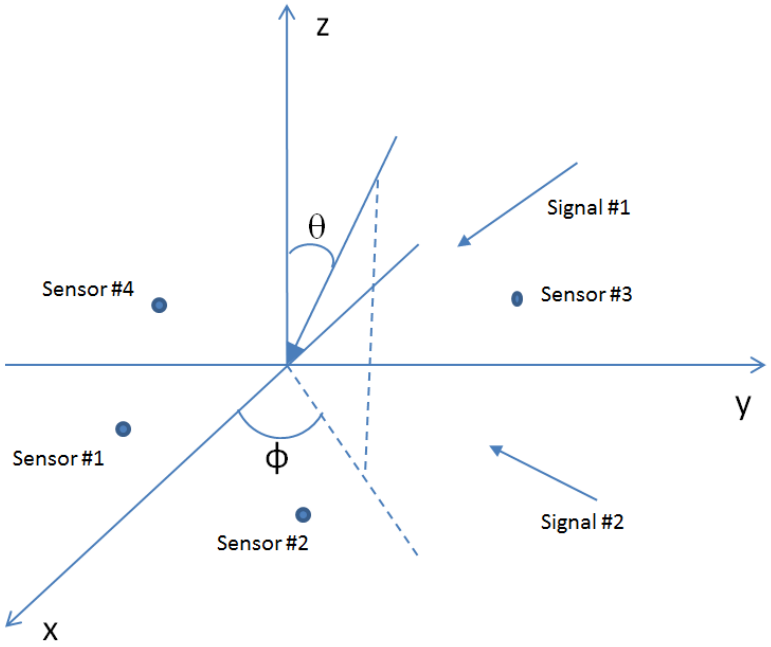

Figure 19. Array with four sensors and two impinging signals [79]

For the impinging signals, we always assume that they are plane waves, i.e. the array is located in the far field of the sources generating the waves and the received signals have a planar wavefront. As an example, a plane wave with a frequency *f* propagating in the direction of the *z*-axis of the Cartesian coordinate system is considered in Figure 20.

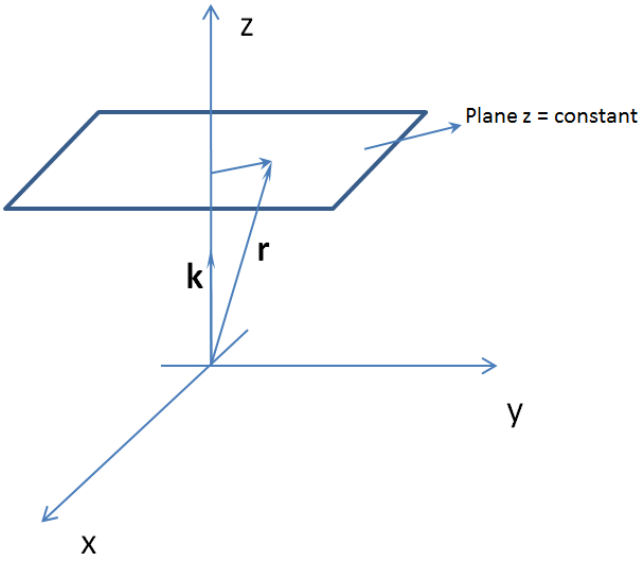

Figure 20. A plane wave propagating in the direction of z axis of Cartesian coordinate system [79]

Where k is the wavenumber, then it can be derived that the time independent phase term is given by [80]:

$$\mathbf{k}^T\mathbf{r} = k(r_x \sin\theta\cos\phi + r_y \sin\theta\sin\phi + r_z \cos\theta)$$

This dependency of the wavenumber is used in an adaptive phased array to steer the beam along desired directions and project nulls to others. [81] depicts a way to arrive at phased arrays using continuous line source antenna.

The different types of beamforming are classified and reviewed in [82] and briefly reported here below.

3.2.1. Weight vector

1) **Fixed weight**: A constant weight is applied to the antenna elements to steer the beam.
2) **Adaptive weight**: The weights are updated dynamically according to the environment projecting high gain beams along desired directions and nulls along undesired ones.

3.2.2. Signal domain

1) **Analogue beamforming**: The analogue beamforming can be either baseband beamforming or RF (Radio Frequency) beamforming depending on whether the phase shifting of the signal is done before upconversion or after upconversion of the signal.
2) **Digital beamforming**: The control signals are from the digital baseband and then processed in the digital signal processor. The beamforming performed this way is more robust owing to the increased processing power on the phase/amplitude by the digital signal processor.

3.2.3. Data handling

1) **Transmit beamforming**: The beamformers are employed between the signal source and the radiating elements to direct the beams along directions predicted by receiver localization.
2) **Receive beamforming**: The beamformers are realized between the antenna arrays and the receiver modules to control the spatial sensitivity of the antenna within its range.

3.2.4. Feedback loop

1) **Open loop beamforming**: The transmitter sends out training sequences to calibrate the channel for phase variations due to multipath and other propagation effects.
2) **Closed loop beamforming**: The receiver estimates the channel and the information is fed back to the receiver.

3.2.5. Bandwidth

1) **Narrowband beamforming**: the weights in this case are frequency independent and therefore the time shifts to constructively add signals can be approximated by corresponding phase shifts.
2) **Wideband beamforming**: Steering vector ceases to be function of signal frequency. Therefore frequency dependent weights need to be determined using tapped delay lines, FIR (Finite Impulse Response) filters etc.

3.2.6. Challenges at mmWave beamforming

1) **Hybrid beamforming multiuser scenario with common scatterers:** mmWave signals owing to their smaller wavelength allow a large number of antennas to be packed into a small size antenna aperture. In conventional digital beamforming each of these antennas are connected to RF chain before digital beamforming is performed, however this is not practical at mmWave frequency considering the large number of antennas involved. Therefore hybrid beamforming is performed which reduces the number of RF chains. Generally the algorithms to date which compute the hybrid beamforming matrix and the analog beamforming matrix do so by assuming mmWave multipath channel model, where propagation paths corresponding to different users have independent angles of arrival at the base station [83]. However, channel measurements for mmWave frequency band show that rough surface/diffuse scattering exists in mmWave, and its diffuse range increases as the wavelength shrinks [84]. This gives rise to common scatterers with similar propagation paths and angle of arrival, which may add severely to the inter user interference. This is an important challenge that needs to be addressed.

2) **Codebook and non-code book beamforming:** Existing dominant analog beamforming schemes can be generally divided into two categories, i.e., the non-codebook beamforming and the codebook-based beamforming. Though non-codebook beamforming offers excellent low complexity designs, they require perfect channel state information (CSI) to be acquired by the Base station (BS) which can be challenging given the limited number of RF chains [85]. The codebook-based beamforming on the other hand has an increased complexity overhead due to search complexity. Higher number of iterations between the BS and the mobile station (MS) leads to greater practical system overhead.

3) **Low rank of the channel matrix:** Generally in mmWave communications, the rank of the MIMO channel matrix tends to be low, due to the presence of a strong LoS component [30].The spatial arrangement of antennas needs to be specifically adjusted to increase the rank of the channel matrix [86]. This is often a challenge. To address this recently spacing between analog beamformers were optimized to maximize the channel matrix rank in a mmWave MIMO environment using a technique- Generalized Spatial Modulation [87].

4) **Range and directional communication:** The smaller wavelength of mmWave signals proportionally enables greater antenna gain for the same physical aperture size of the antenna [82]. And therefore the higher frequencies of mmWave signals do not decrease the free space propagation loss as long as the antenna area remains fixed and proper beam forming is performed. The gain obtained in the phased array scenario for an array of N antennas is given by [82]

$$\text{Gain(array)} = \text{Gain(single antenna)} + 20\log_{10}(N)\ \text{dB}$$

Obtaining high directional beamforming gains can completely compensate for and further reduce the increase in the path loss with frequency. This however poses a particular challenge in the design of synchronization and broadcast signals used in initial cell search. These signals need to be scanned over a range of angles and this spatial searching, owing to highly directional beam, results in delay in BS detection in handovers.

5) **Shadowing:** mmWave signals are very prone to shadowing. Materials such as brick, human body can attenuate signals by 40-80 dB [82]. A correct assessment of the shadowing environment and accounting for the attenuation loss by increasing the beamforming gains offers significant challenge in realizing beamforming networks.
6) **Rapid channel fluctuations:** For a given mobile velocity, channel coherence time is very small in the mmWave range. The Doppler spread at 60 km/hr at 60 GHz is over 3 kHz [133] and hence the channel will change in the order of hundreds of microseconds. To keep in pace with this it is indeed challenging to design low latency beamforming networks than can accommodate the rapidly fluctuating channel state.

7) **Fully Digital vs Mixed Digital/AnalogueSolutions:** Fully digital beamforming methods require one RF chain per antenna. The hybrid/mixed digital/analogue solution divides signal processing into digital and analogue domains in order to support multi stream and multi user. A hybrid transmit full array beamformer is shown in Figure 21. The hybrid beamforming consists of fewer number of RF chains with digital processing in the baseband or RF domain followed by analogue processing to obtain antenna beamforming gains [82]. The challenges in hybrid/mixed beamforming when compared to fully digital are listed below:
   - **Number of RF chains and analogue phase shifters**: This needs to be arrived at optimally considering the multiplexed and antenna elements. The performance of the fully digital beamforming is targeted keeping in view the hardware cost and power constraints.
   - **Channel estimation**: Channel estimation is a key factor in any type of beamforming or massive MIMO related processing. The limited number of RF chains as compared to the number of antenna elements in hybrid beamforming presents a bottle neck in channel estimation. Thus channel estimation in hybrid beamforming is an optimization problem that identifies optimal RF transmit receive pairs to maximize mutual data.
   - **Beam training and feedback**: Reference signal sequences designed for joint baseband and RF beamforming in order to reduce the feedback and training overhead can yield low complexity power efficient implementations.

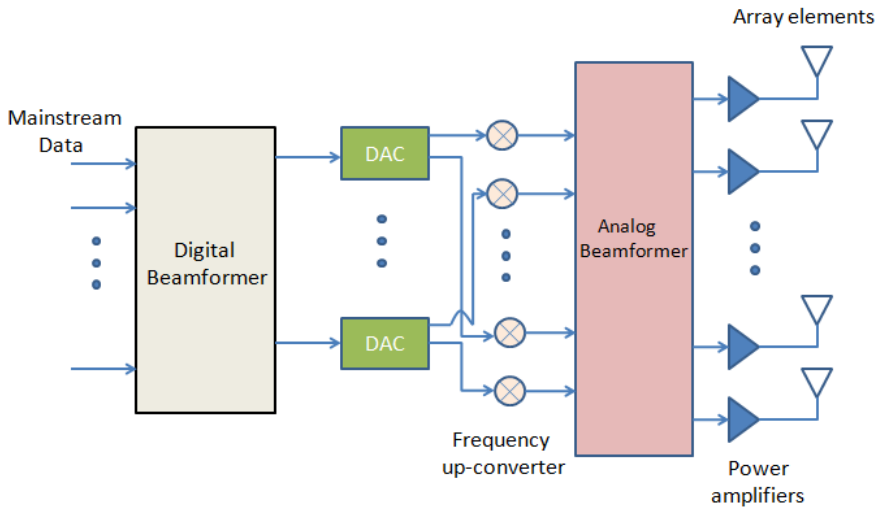

Figure 21.Typical hybrid beamforming transmit architecture for a full array [82]

3.3. State-of-the-art assessment of mmWave antennas

To summarize what was discussed above, millimetre wave spectrum comes inherently with a large bandwidth and its LOS propagation limitation can be overcome by high gain beamforming. A recent study has shown the mmWave communication to be useful for cellular communications practically [88]. Advanced methods of mmWave beamforming that employ both the advantages of analogue and digital beamforming together called hybrid beamforming are being used recently [82]. The papers [89] and [90] provide a broad overview and survey of the large scale MIMO systems and [82] considers a detailed review of mmWave beamforming to date. It identifies the main drawbacks of mmWave like increased path loss and discusses about high gain beamforming techniques to overcome this. The different ways of beamforming like digital, analogue or their hybrid are discussed along with the emerging trends in mmWave beamforming. To perform hybrid beamforming, analogue phase shifters are generally used. An interesting proposition is to change to switches that consume less power and have a low complexity [91].

Antenna designs for these massive MIMO arrays have been proposed recently keeping the mmWave band in consideration. A selection of these antennas is presented in the section below.

- **Tilted Combined Beam Antenna:**

One such antenna design [92] is the tilted combined beam antenna that provides a tilted radiation in the elevation plane operating around the 28 GHz band, as shown in Figure 22. Instead of using array to provide the elevation angle tilt, two radiating elements are used to produce the tilted beam. One is a group of microstrip patches and the other is a waveguide aperture. A relatively high antenna gain of 7.4 dBi even with wide beam spreading across the azimuthal plane can be obtained. The tilted beam is obtained without using antenna arrays or active RF components. Of the two radiating elements one is for a wide beamwidth on the azimuthal plane and the other is for strong radiation in the elevation plane. To obtain a high gain beam in the desired tilted direction the spacing between the two radiators is optimized. This antenna design is of interest in multilayer sectoring methodology which is a new way of sectoring cell site based on radius.

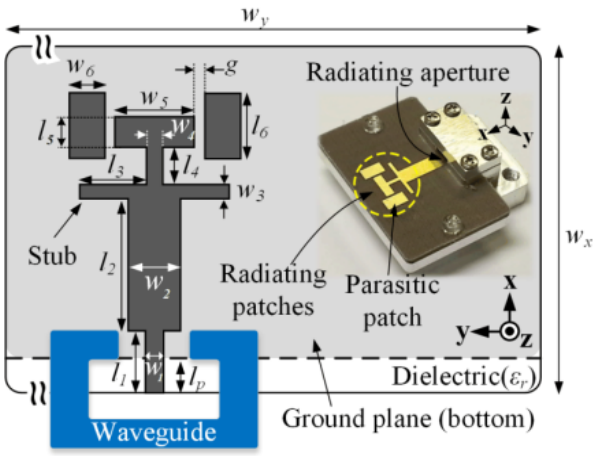

Figure 22.Tilted combined beam antenna [92]

- **Turning Torso Antenna:**

Dual slant polarization is of key importance in massive MIMO antenna arrays owing to the ease with which the polarized components can be resolved at the receiver. [93] proposed a design termed the turning torso antenna shown in Figure 23, which uses three orthogonal hexagonal stacked rings operating at 3.7 GHz. The arrangement allows 18 beams along the entire 360°range with a gain of 16.6 dBi.

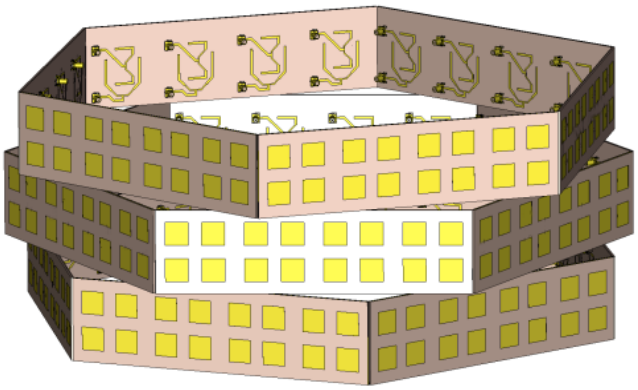

Figure 23. Turning torso antenna [93]

- **Improved XPD Antenna:**

Another dual polarized base station antenna element [94] is shown in Figure 24, which uses four parasitic elements placed in a square contour to increase the cross polar discrimination (XPD). The principle of wide beamwidth and high XPD was investigated.

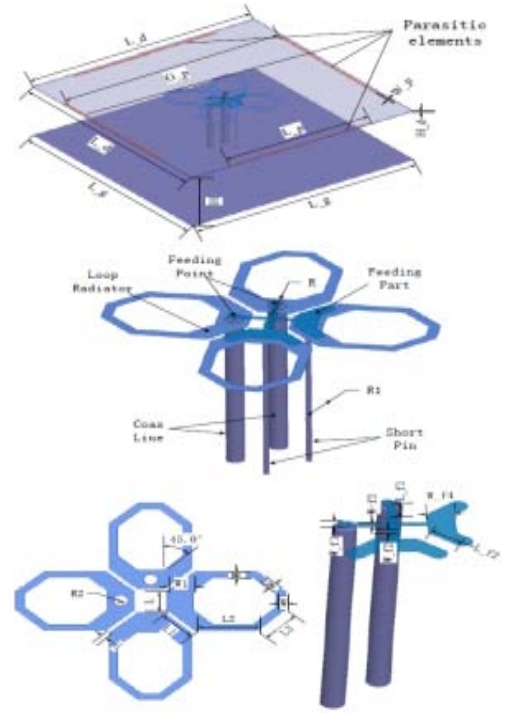

Figure 24.Improved XPD antenna [94]

- **Double Dipole Antenna:**

Another antenna design as described in [95] and shown in Figure 25 is a two folded dipole fed in phase with a CPW transmission line with four parasitic patches surrounding it to enhance directivity and minimize surface waves. It operates at 122 GHz with a gain of 11 dBi.

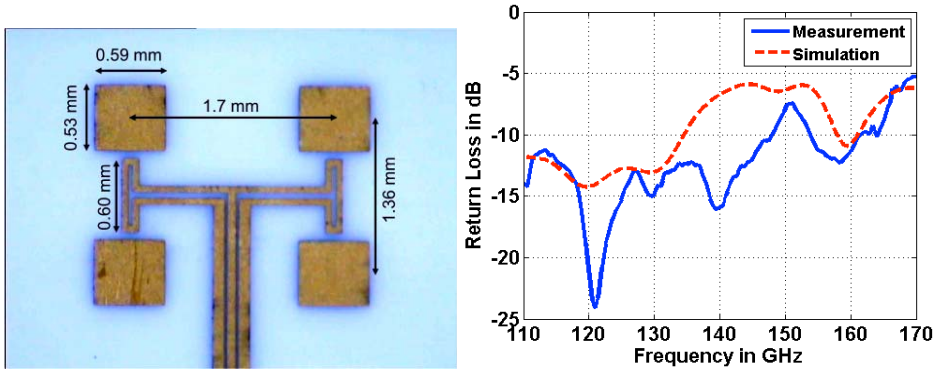

(a) (b)

Figure 25. Double dipole antenna at 122 GHz with return loss [95]

- **SIW Antenna Array:**

A work that focuses on substrate integrated waveguide technology (SIW) is shown in Figure 26. SIW is relatively easy to integrate and compact. It also provides a low loss feeding network to the antenna. The antenna in [96] operates in the 76-86 GHz E-band with antenna design made of SIW technology. It has a high gain of up to 15 dBi and wide beamwidth of 25 degrees in E plane and 30 degrees in H plane. It uses the mainstream PCB process and has four metal layers and three substrate dielectric layers. It is a low cost steerable E band antenna with a SIW feed network made of H and T junctions to feed the antenna element.

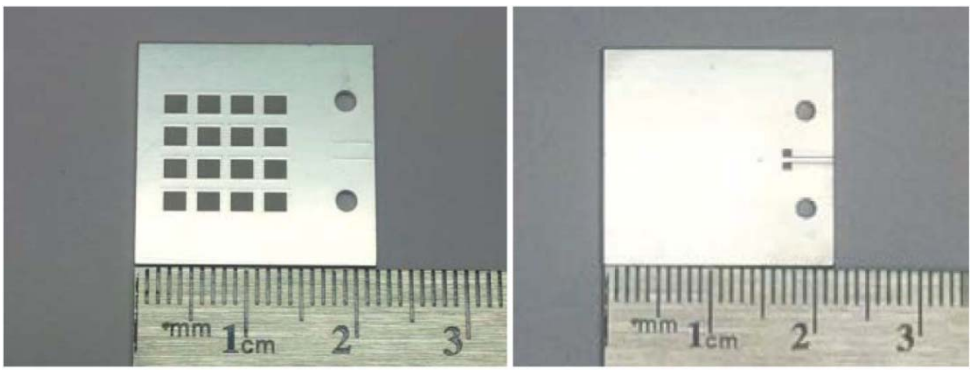

Figure 26. SIW antenna array [96]

- **Inkjet Printed Multilayer Yagi-Uda Antenna:**

The antenna design for the large scale MIMO needs to be scalable. The cost of fabrication and deployment at mmWave frequencies limits this from being feasible, especially when designing3D antennas. A recent fabrication technique that has been gaining momentum owing to its low cost, scalability and environment friendliness is inkjet printing. [97] has proposed a Yagi-Uda antenna with

gain of 8 dBi in the 24.5 GHz frequency range using inkjet printing methodology shown in Figure 27. It further demonstrates the technologies potential for integration with on-chip and on-package fabrication schemes. It also shows a good RF integrity of both the metallic and dielectric ink materials within the inkjet printing process. Multi-layer material deposition is used to realize the 3D antenna structure including realization of the dielectric substrate to support the microstrip to slotline transition. One major advantage of this technology is the ease of post process deposition of antennas onto any rigid or flexible active/passive circuit topology. It can be seen this brings in an extra degree of freedom - blending into the pre-existing design.

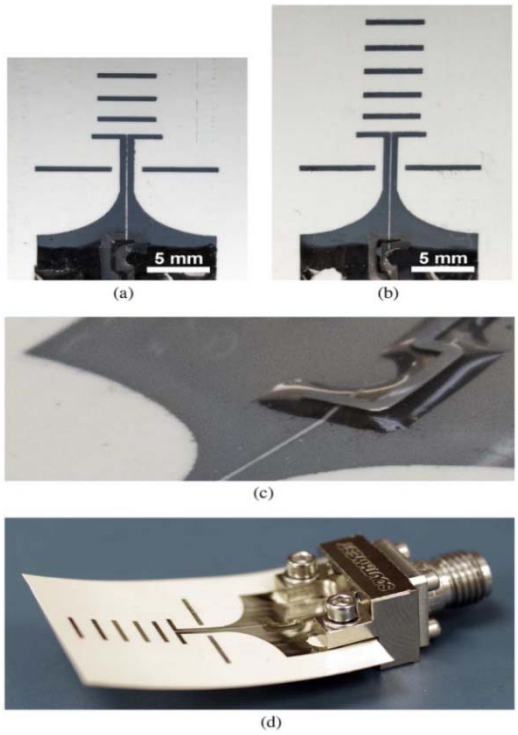

Figure 27. Inkjet printed multilayer YagiUda antenna (a) 3 director elements (b) 5 director elements (c) microstrip to slotline transition (d) slightly bent substrate antenna [97]

- **Aperture Coupled Magnetic Electric Dipole Antenna:**

Recently mmWave communication antennas have been designed using the patch or the slot. These designs have narrow impedance bandwidth and radiation pattern bandwidth. To enhance this, design with SIW and dual polarization incorporated in it is proposed in [98] and shown in Figure 28. An aperture coupled magneto electric dipole is presented that is designed over three layer of substrate, with a four element patch antenna built on the top layer aided by a cross slot to enhance impedance matching. This structure is further controlled by a beamforming network made of a 90°coupler. The beamforming network allows steering the beam along 2D and can be extended to a beamswitching network by incorporating switches. The use of magneto electric dipole concept reduces the back-lobes and ensures a good front-to-back ratio of 20 dB. The antenna and the array operate at 60 GHz and several other contemporary similar design techniques employ slots, patches, dipoles and cavity to realize multibeams along 1D and 2D. The 1D multibeams are along the azimuthal or elevation plane like fan beams with narrow beamwidths cast simultaneously along the azimuthal plane, while not covering the other dimension. The 2D multibeams jointly covers

azimuthal and elevation dimensions. These techniques mostly operate in the linear polarization and have an impedance bandwidth ranging from 12-19%. The design has an impedance bandwidth of 22%.

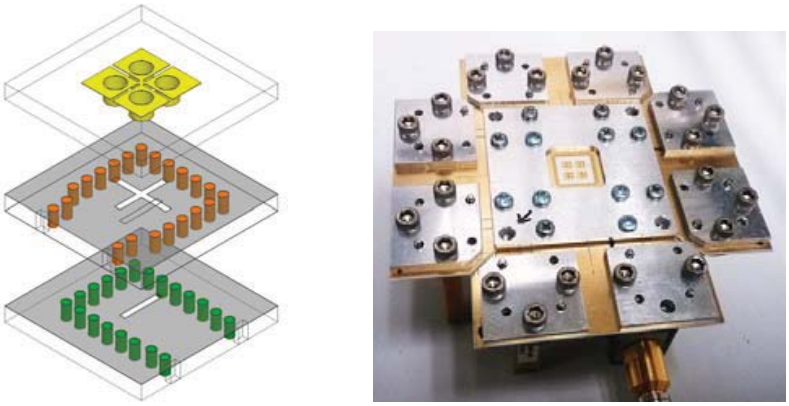

Figure 28. Geometry of the aperture coupled magnetic electric dipole antenna and the fabricated prototype [98]

- **Ka Band CP Array:**

Circular polarization has been generally treated next to dual polarization in cellular communications, however it is used in anti-multipath interference and good polarization matching. A wideband, high efficiency, circular polarized planar array antenna operating at Ka band is presented in [99] and its exploded view is shown in Figure 29. The radiating element is a cross slot with four parasitic patches. The aperture coupling technique is used by the array and is fabricated using PCB. A gain of 18 dBiC in the frequency band of 26-30 GHz is obtained.

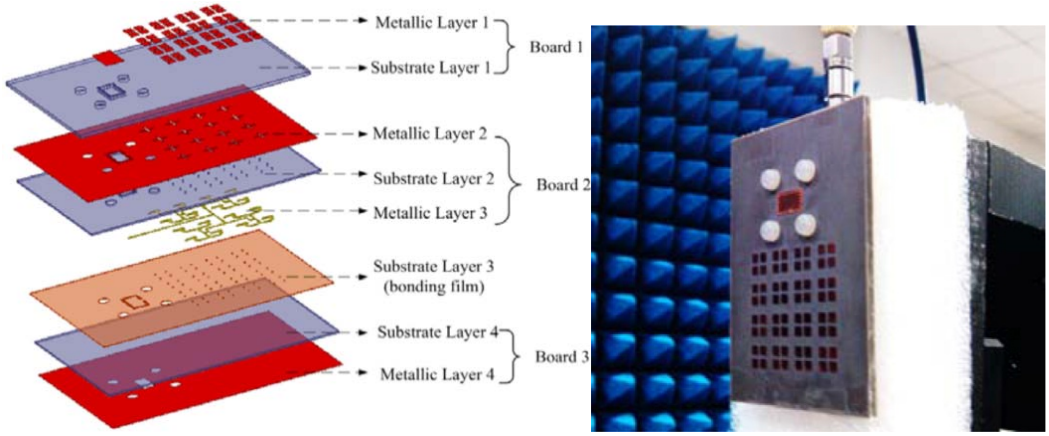

Figure 29. 3D configuration of the Ka band CP array and fabricated prototype [99]

- **Conformal Antenna Array:**

While mmWave beamforming is majorly concerned with high gain beamforming to improve data rates, beamswitching employed at pico or femto cell sites to switch the beam along different UEs would be an added advantage. Millimeter wave beamswitching has been presented in [100] using a conformal antenna array. It consists of 3 antenna arrays of 16 patch elements in each array operating at 61 GHz. A single pole three throw (SPTT) switch controls the beam switching. The fabricated antenna array is shown in Figure 30.

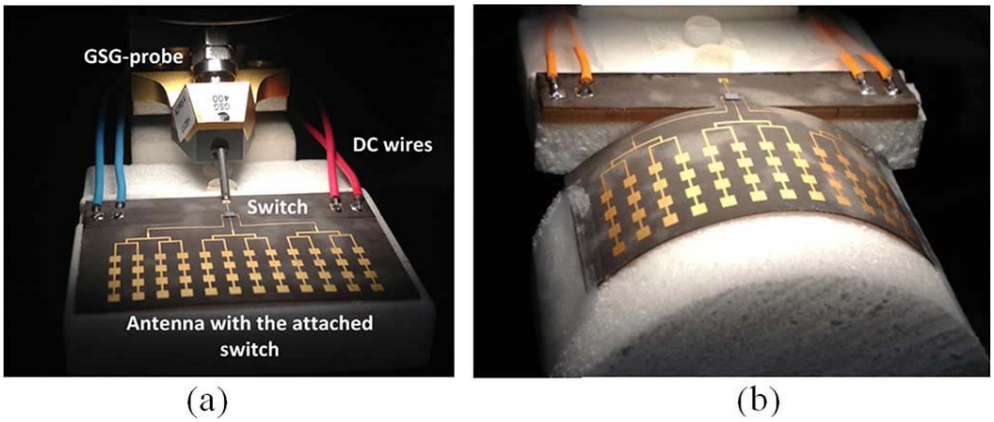

Figure 30. Planar prototype and the convex prototype of the conformal array [100]

- **Planar Aperture Antenna:**

A design that uses differential feeding to obtain high gain circular polarization at mmWave frequency is proposed in [101]. It has a wide bandwidth and can be fabricated using PCB process that makes the antenna easy to integrate to differential circuits. The antenna consists of open cavity made of metalized vias which encloses loop like strip fed differentially [101] and is shown in Figure 31. The aperture´s E field together with the travelling wave current give rise to the circular polarization. The antenna operates at 60 GHz and achieves 3 dB AR (Axial Ratio) of 16.7% while providing a peak gain of 14.6 dBi. The antenna is low cost and has a low profile as it can be realized on a single layer laminate and is fabricated using standard planar circuit technology. The differential feeding scheme of the antenna further eliminates the use of baluns as these can be integrated into the differential mmWave circuits directly and effectively.

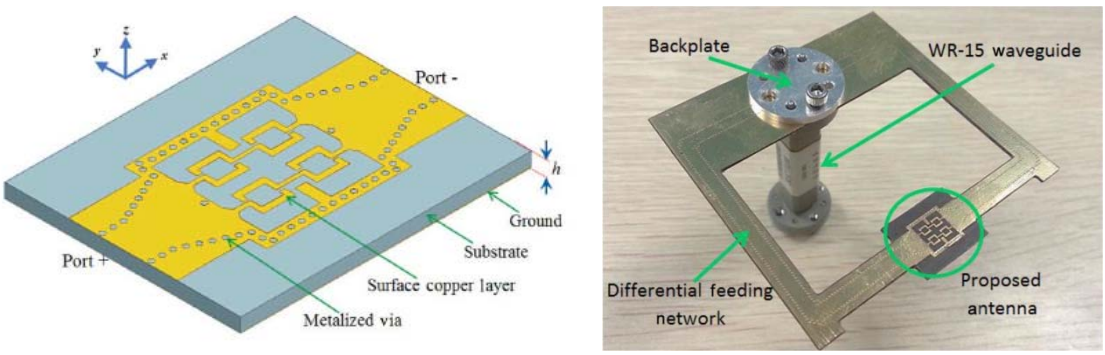

Figure 31. Model and fabricated prototype of the planar aperture antenna [101]

A comparison of previous antennas is shown in Table 3:

Table 3. Comparison of different antenna types based on gain, polarization and bandwidth

Antenna type	Frequency Band	Gain (dBi)	Polarization	Impedance Bandwidth
Tilted combine beam antenna	27.2 GHz - 28.7 GHz	7 .4 dBi	Linear	5.4%
Hexagonal stacked ring	3.64GHz-3.8 GHz	16.6 dBi	Dual	3.6%
Improved XPD antenna	1.7-2.7 GHz*	8.9 dBi	Dual	45%
Inkjet printed multilayer YagiUda antenna	21-27 GHz	8 dBi	Linear	25%
Aperture coupled magneto electric dipole	53.4-71.8 GHz	12.5dBi	Dual	29.3%
Ka band array	26.4-30.3 GHz	17.4dBic	Circular	13.7%
Conformal array	57-63 GHz	18.8 dBi	Linear	10%
Differentially fed planar aperture antenna	57-66 GHz	14.6 dBi	Circular	16.1%

**Antenna operating in microwave band shown as it offers a technique to better cross polarization discrimination that could hold as well in mmWave band*

- **SIW Arrays:**

Considering the cellular communication link, antennas need to be designed for backhaul link and access point to UE link. High gain and directive beams and quasi optical systems are needed. SIW fed slot array [102], SIW fed chain array [103] are two examples shown in Figure 32to obtain high gain narrow beams. The SIW fed slot array has a peak measured gain of 33.1 dBi at 61.5 GHz with an efficiency of 56.8% while the SIW fed chain array has a radiation efficiency of 74%.

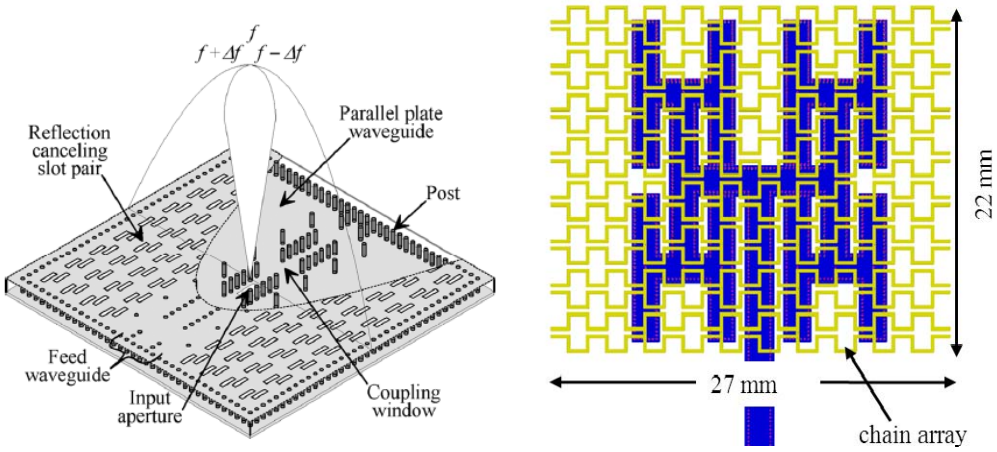

Figure 32. SIW arrays: SIW fed slot array 0and SIW fed chain array [103]

For the access point to UEs, beamswitching or beamsteering antennas are required owing to the mobility of UEs. Other than the SIW arrays used for the backhaul link, the 60 GHz beam switched

receiver that is presented in [104] uses GaAs switches on a liquid crystal polymer substrate; the active peak gain is 27.5 dBi. Beam switched antennas have also been realized using Rotmanlens [105] and integrated reflector systems [106].

3.4. Research roadmap

The present section outlines our research objectives in project 5Gwireless.

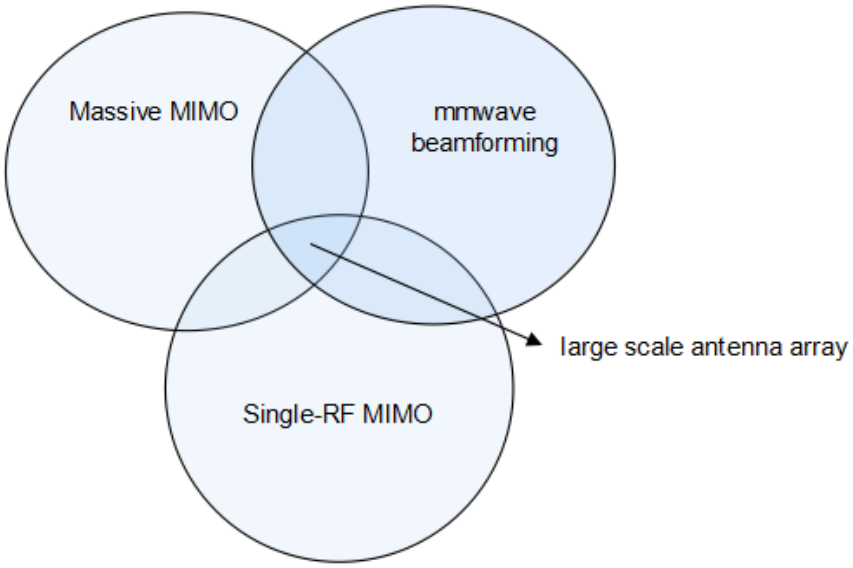

Figure 33. Venn Diagram of Interdependency

The aim to realize large scale antenna arrays is three fold. It involves design of massive MIMO, single RF MIMO and use of mmWave beamforming with high gains. Massive MIMO can be realized using analogue or digital beamforming or a hybrid combination of the two. Single RF MIMO can be realized using techniques like parasitic/beamspace technology or spatial modulation. There are areas of overlap between the single RF and massive MIMO w.r.t. mmWave beamforming as shown in the Venn diagram in Figure 33. The number of antennas in the Massive MIMO antenna array that can do without the RF chains will depend on number of antennas that a single RF chain can serve efficiently while maintaining the high gains required by mmWave beamforming. The large number of antennas and the number of antennas served by a single RF chain needs to reach an optimal trade-off. It is aimed to have an antenna prototype each for the massive MIMO, the single RF MIMO and mmWave high gain beamforming fields.

3.5. Conclusion

The review reveals that mmWave band is promising for high data rate communications when antennas designed for mmWave band are used in conjunction with high gain analogue and digital beamforming. The antenna design at these frequencies is guided mainly by alleviating the array effects in large scale array antennas by employing customized elements towards the edges of the

array. For antenna design, parameters like the polarization ports isolation, gain, possibly dual slant polarization, feed network, or possibility of attaining super directivity by packing the antenna elements close, can be investigated. Antenna array configurations in 3D like the cylindrical or spherical have potential to offer 360 degree beamforming which is ideal in a small cell or pico-cell environment. Multilayer sectoring is a key area to better 5G deployments. It uses different elevation angles at the base station to cast different concentric beams, centered at the base station, while maintaining the same azimuthal beamwidth. It needs antenna array configurations that could steer the beam efficiently with respect to the beamwidth along the elevation direction as well. This would mean maintaining a balanced approach in the antenna array design along both the azimuth and elevation.

4. Signal processing challenges

MIMO technology has been intensively investigated in the last decades because it is able to provide a spectral efficiency proportional to the minimum number between the transmitting and receiving antennas in a point-to-point transmission. Nevertheless, these gains impose an increase of: a) the required hardware complexity (i.e. number of RF chains), b) energy consumption, and c) signal processing (precoder/receiver design), [107].

Recently, very large MIMO has become a very active research field thanks to their benefits in terms of system design [107]. It turns out that the transmitted power per antenna is inversely proportional to the total number of antennas, so that low power amplifiers can be considered, in contrast to conventional MIMO systems. Because of the large number of antennas, some random variables like the channel matrix tend to become deterministic, matrix operations like inversions can be done faster, thermal noise can be averaged and the system becomes limited by interference. Nevertheless, one of the main drawbacks is how the channel state information is acquired. In general, the transmitter (base station) sends one training pilot signal per antenna, so that every user can estimate the channel state and feedbacks to the base station. Since there are so many antennas, such approach is not feasible. Consequently, very large MIMO systems are deployed in Time Division Duplexing (TDD) in order to exploit the *channel reciprocity*. Hence, base station estimates the channel from transmissions done by the users.

Another research direction adopted in the last years for enlarging the available spectrum devoted for wireless communications is to work in the millimeter wave band (26-70 GHz) where there is a huge unused spectrum, several hundreds of MHz, compared with the current available at the centimeter band (2-6 GHz). It is widely known that the channel pathlosses are significant in the mmWave band, but this can be combated by using MIMO technology. The natural question is to know if the signal processing techniques developed for conventional MIMO and very large MIMO systems at the cmWave band are suitable for the mmWave band.

The answer is that in general this is not possible because the signal processing is dependent on the operational frequency band, see section II of [108]:

- *Hardware constraints imposed by working in high frequency and large bandwidth*
  While at lower frequencies all the signal processing can be carried out in the baseband, mmWave-based systems need to work with a separate RF chain and data converter for each antenna. The practical implementation of the power amplifier (PA) or the low noise amplifier (LNA) is challenging. Furthermore, all antennas elements are placed in a small area for avoiding grating lobes, so that a complete RF chain per antenna is not allowed.

- *Power consumption*
  The power consumption of the different elements in the transmitter/receiver chain like the PA, analog-to-digital converters (ADCs) or data interface cards increases at the mmWave-band, see [109] and table I of [108]. Additionally, the digital signal processing demands to

work with many parallel gigasamples per second data streams, demanding high power consumption.

- *Channel models in mmWave and cmWave are different*
  In the mmWave the channel is sparse in time and angle of arrival/departure, i.e. the channel matrix is always rank-deficient. This property can be seized for simplify the signal processing techniques to be applied at the transmitter or receiver side.

- *Large arrays can be employed at transmitter and receiver side*
  Because of the operational frequency, it is possible to pack many antennas in a small area. In contrast, when we work at the cmW band, only base stations are allowed to have many antennas, while mobile terminals tend to have at most 2.

- *Frequency selective channel*
  The use of beamformers (for compensating the pathlosses) allows reducing the delay spread of the channel, but since it is expected to work with a larger band than those systems in the cmWave band, the channel becomes frequency selective [110].

- *Doppler*
  Let us emphasize that the use of mmWave band is envisioned for small cell areas (up to 200 m), where served users are assumed to have a low velocity. However, Doppler effect might be significant because it depends also with the carrier frequency. It is expected that the CSI (Channel State Information) should be updated similarly to the current MIMO systems in lower frequencies with Macro cells where a typical Doppler is 200 Hz.

- *Time variations*
  Sensitive phase and frequency tracking algorithms are important because time variations due to the carrier and frequency offsets and phase noise in the RF up- and down-conversion impose significant losses.

In the following we review the current state-of-the art in terms of signal processing for mmWave that is surveyed in part in [108]. In section 4.1 we present the different approaches that have been considered for the MIMO transceiver design. At the transmitter side, there are two approaches: *only-analog beamforming* (section 4.1.1) or *hybrid analog-digital beamforming* (section 4.1.2). The latest approach allows applying digital signal processing at the baseband. Additionally, in section 4.1.3 we review how including *low-precision ADCs* with low-power consumption impacts on the total system design elucidating a trade-off between the achievable rate and energy consumption as a function of the number of bits of ADC. The other topic where signal processing plays an important role is for the channel estimation. There are two approaches: *codebook beamtraining* (section 4.2.1), where a protocol for transmitting different codewords is used and the users do not estimate explicitly the channel, *and sparse channel estimation* (section 4.2.2) where techniques based on compress sensing are considered for estimating the channel thanks to the sparsity properties of the mmWave channel.

4.1. MIMO Transceiver Design

The main drawbacks of working at the mmWave band presented previously have motivated the investigation of several MIMO architectures. In the literature there are 3 important aspects to take into account: i) Ratio between the number of transmit/receive antennas and the RF chains, ii) type of ADC at the receivers, and iii) existence of only-analog RF precoding/combining or hybrid analog-digital precoding. It turns out that there are more parameters to configure than working in lower frequencies.

In this regard Figure 34 depicts a general architecture for the MIMO mmWave transceivers with N_t transmitting and N_r receiving antennas, L_t and L_r RF chains at the transmitter and receiver side, respectively, and N_s streams. The signal processing applied for the precoding is done with the filters $\mathbf{F}_{BB}, \mathbf{F}_{RF}$ at the baseband and RF, respectively, while the signal processing at the receiver side is considered in the desing of combiners $\mathbf{W}_{BB}, \mathbf{W}_{RF}$, see Figure 34. Analog-based systems work with $\{N_s = 1, L_t = L_r = 1\}$, while the hybrid precoding systems consider $\{N_s < L_t \leq N_t, N_s < L_r \leq N_r\}$.

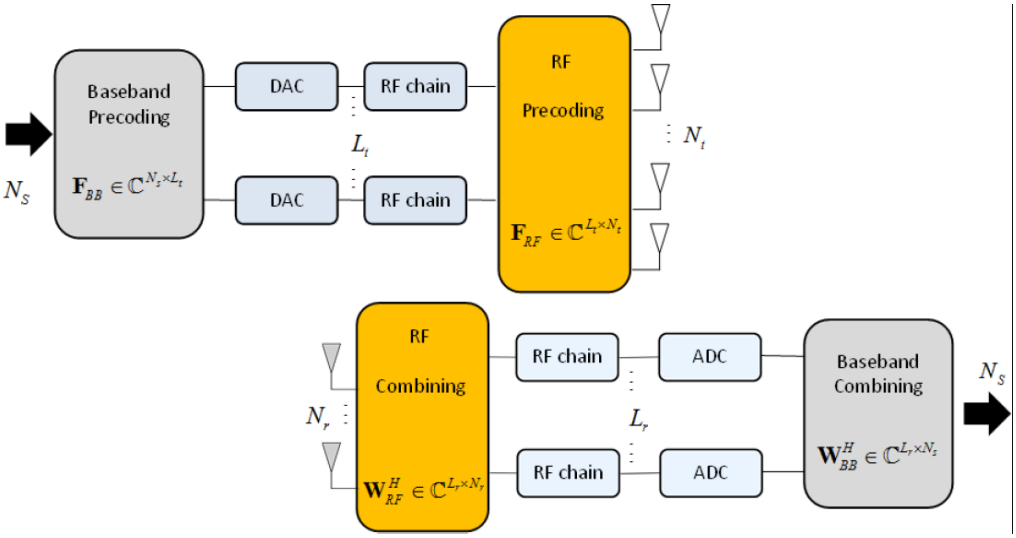

Figure 34: General MIMO transceiver architecture for mmWave systems

Notice that conventional MIMO architectures for lower frequencies tend to consider $\{N_s \leq \min(N_t, N_r), L_t = N_t, N_r = L_r, \mathbf{W}_{RF} = \mathbf{F}_{RF} = \mathbf{I}\}$. Hybrid architectures have been considered for lower frequencies, however their precoder design does not seize the channel sparsity available at the mmWave band. In the following we review the signal processing required for analog beamforming and hybrid analog-precoding in section 4.1.1 and section 4.1.2, respectively. In terms of analog beamforming the typical schemes are based on phase shifters (section 4.1.1.1) or continuous aperture phased MIMO (section 4.1.1.2). On the other hand, for the hybrid analog-digital precoding we study spatially sparse-based, codebook-based and CAP-MIMO based precoding in sections 4.1.2.1, 4.1.2.2, and 4.1.2.3, respectively. Furthermore, sections 4.1.2.4 and 4.1.2.5 are devoted to explore the precoding in the multi-user case and in the frequency-selective channel. Finally, section 4.1.3 describes the challenges on the mmWave-based systems when low-precision baseband ADCs are considered with the objective of power saving.

4.1.1. Analog beamforming

Analog beamforming, introduced in section 3.2, is the simplest MIMO implementation. In this approach the antenna elements are connected to a single RF chain, i.e. $\{N_s = 1, L_t = L_r = 1, \mathbf{F}_{BB} = \mathbf{W}_{BB} = 1\}$ in Figure 34. Signal processing optimization tries to find the best beamformers at the receiver and transmitter side.

The principal shortcoming of this approach is that it only supports single-user and single-stream transmission, and it is highly dependent on the beam training algorithms. The narrowband channel in line-of-sight conditions can be modelled as,

$$\mathbf{H} = \beta \mathbf{a}_r(\theta_r)\mathbf{a}_t^H(\theta_t) \quad (1)$$

where $\mathbf{a}_r(\theta_r), \mathbf{a}_t^H(\theta_t)$ denote the vector in the receiver's and transmitter's manifold corresponding to the angle of arrival and departure, respectively, and β is the normalized channel gain. The discrete-time model for the received signal is

$$y = \sqrt{\rho}\mathbf{w}_{RF}^H \mathbf{H}\mathbf{f}_{RF} s + \mathbf{w}_{RF}^H \mathbf{n} \quad (2)$$

where ρ stands for the average transmitted power per symbol and $\mathbf{n}$ is the noise vector. The precoder and receive combining to be optimized are given by $\mathbf{w}_{RF}, \mathbf{f}_{RF}$, notice that the matrices defined in Figure 34 become a column vectors in this case.

The beamfomers can be implemented by means of phase-shifters (section 4.1.1.1) or CAP-MIMO (section 4.1.1.2).

4.1.1.1. Phase shifters

In this case the analog beamforming is done by means of digitally controlled phase shifters. This is an approach considered in IEEE 802.11ad. Signal processing optimization is applied to design the phase shifter weights to a given criterion defined beforehand, i.e. maximizing the signal-to-noise ratio of the desired signal. The optimization is challenging because of the use of quantized phase shifts without any amplitude adjustment, so that fine tuning the beams and steering nulls is not easy. An illustrative example of the analog beamforming design is provided in [111].

In case of using an uniform linear array (ULA) with elements spacing d, the array manifold with possible angle of arrivals in $\mathcal{T}$

$$\mathcal{A} = \left\{ \mathbf{a} : \mathbf{a} = \left[1 \quad \exp\left(j2\pi \frac{d}{\lambda} \sin(\theta) \right) \ldots \exp\left(j2\pi (M-1) \frac{d}{\lambda} \sin(\theta) \right) \right]^T \text{ for } \theta \in \mathcal{T} \right\} \quad (3)$$

An analog beamforming pattern is generated with a RF phase-shifter with q bits per element, so that each antenna phase takes one value among 2^q set of quantized phases,

$$\varphi_m \in \left\{ 0, 2\pi\left(\frac{1}{2^q}\right), 2\pi\left(\frac{2}{2^q}\right), \ldots, 2\pi\left(\frac{2^q - 1}{2^q}\right) \right\} \quad (4)$$

The transmitting and receiving beamformer are written as,

$$\mathbf{f}_{RF} = \frac{1}{\sqrt{M}}\left[1 \ \exp\left(j\varphi_1^t\right) \ldots \exp\left(j\varphi_{M-1}^t\right)\right]^T$$
$$\mathbf{w}_{RF} = \frac{1}{\sqrt{N}}\left[1 \ \exp\left(j\varphi_1^r\right) \ldots \exp\left(j\varphi_{N-1}^r\right)\right]^T \quad (5)$$

The beamformers can be obtained as a solution of the following optimization problem,

$$(P_1): \quad \underset{\{\varphi_i^r\},\{\varphi_i^r\}}{\text{maximization}} \quad \left|\mathbf{w}_{RF}^H \mathbf{H}\mathbf{f}_{RF}\right|^2 \quad (6)$$

4.1.1.2. Continuous aperture phased (CAP) MIMO

In contrast to previous section, it is possible to implement the analog beamformer using a high resolution discrete lens array (DLA) to enable a quasi-continuous aperture phased-MIMO operation, (CAP -MIMO) [112]. The lens is excited by feed elements on an associated focal surface, in this particular case, the data streams. The signal propagation from the focal arc to the aperture affects a continuous Fourier transform, that can be approximated by a discrete Fourier transform matrix corresponding to critical sampling of the aperture and the focal arc.

$$\mathbf{U}_a(l,m) = \frac{1}{\sqrt{n}}\exp\left(-j\frac{2\pi lm}{n}\right), \quad l \in \mathcal{I}(n), m \in \mathcal{I}(n) \quad (7)$$

where l represents the samples on the aperture (spatial domain) and m denotes the samples on the focal arc (beamspace). Figure 35 compares different dielectric lenses.

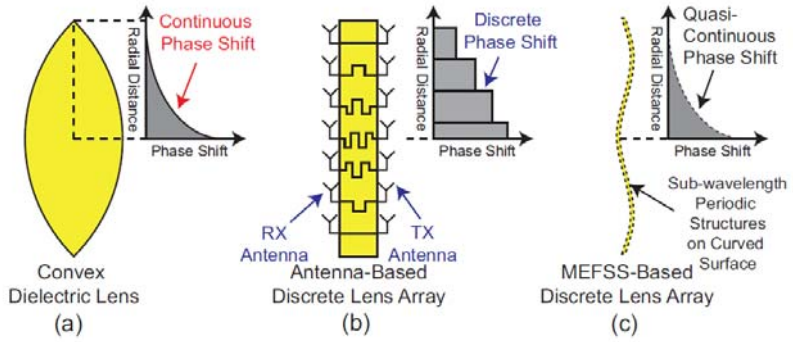

Figure 35: Comparison between different dielectric lenses: a) traditional microwave lens composed of arrays of receiving and transmitting antennas, b) proposed conformal metamaterial-based microwave DLA using the sub-wavelength periodic structures shown in c). Original figure from [112]

4.1.2. Hybrid analog-digital precoding

This approach enhances the previous analog beamforming technique by introducing additional digital signal processing capabilities at the baseband. In such a case the lack of precision of analog beamforming can be alleviated at the cost of increasing the hardware complexity. It is possible to

employ spatial multiplexing N_s streams using L_t and L_r RF chains at the transmitter and receiver side, respectively, see Figure 34.

The received signal is given by,

$$\mathbf{y} = \sqrt{\rho}\mathbf{W}^H\mathbf{H}\mathbf{F}\mathbf{s} + \mathbf{W}^H\mathbf{n} \tag{8}$$

where $\mathbf{s} \in \mathrm{C}^{N_s \times 1}$ are the transmitted symbols and $\mathbf{W} \in \mathrm{C}^{N_r \times N_s}, \mathbf{F} \in \mathrm{C}^{N_t \times N_s}$ take into account the RF and base band (BB) precoders and combiners.

$$\mathbf{W} \triangleq \mathbf{W}_{RF}\mathbf{W}_{BB}, \quad \mathbf{F} \triangleq \mathbf{F}_{RF}\mathbf{F}_{BB} \tag{9}$$

with $\mathbf{W}_{RF} \in \mathrm{C}^{N_r \times L_r}, \mathbf{W}_{BB} \in \mathrm{C}^{L_r \times N_s}$ and $\mathbf{F}_{RF} \in \mathrm{C}^{N_t \times L_t}, \mathbf{F}_{BB} \in \mathrm{C}^{L_t \times N_s}$, being L_r, L_t Lt the number of RF chains at the receiver and transmitter respectively.

Because of the transmitter and receiver structure imposed by this approach, in addition with the constraints to be met, the optimization of these variables is very challenging because transmit precodiers and receive combinersare written as a product of matrices, (9).

In the sequel we review different types of precoding schemes based on the spatial sparsity of the channel (sections 4.1.2.1), codebook design (4.1.2.2) and CAP-MIMO in (4.1.2.3). Additionally it is described the extension to multi-user case and frequency-selective fading channel in sections 4.1.2.4 and 4.1.2.5, respectively. The precoder design is dependent on the precision assumed in the ADCs at receiver side.

4.1.2.1. Spatially sparse-based precoding

The sparse-scattering structure of the mmWave channel is considered in [113] to design the analog RF and digital baseband precoders as the solution of a sparsity constrained matrix reconstruction problem. The proposed algorithm takes into account an optimal unconstrained precoder as an input and finds linear combinations of analog RF and baseband precoders. At the receiver side, it is shown that MMSE combiners can be seen as a sparse approximation problem.

$$(P_2): \begin{cases} \left(\mathbf{F}_{RF}^{opt}, \mathbf{F}_{BB}^{opt}\right) = \arg \min_{\mathbf{F}_{RF}, \mathbf{F}_{BB}} \left\|\mathbf{F}_{opt} - \mathbf{F}_{RF}\mathbf{F}_{BB}\right\|_F \\ \quad s.t. \quad \mathbf{F}_{RF} \in \mathcal{F}_{RF} \\ \quad \left\|\mathbf{F}_{RF}\mathbf{F}_{BB}\right\|_F^2 = N_s \\ \left(\mathbf{W}_{RF}^{opt}, \mathbf{W}_{BB}^{opt}\right) = \arg \min_{\mathbf{W}_{RF}, \mathbf{W}_{BB}} \left\|E\left[\mathbf{y}\mathbf{y}^H\right]^{\frac{1}{2}}\left(\mathbf{W}_{MMSE} - \mathbf{W}_{RF}\mathbf{W}_{BB}\right)\right\|_F \\ \quad s.t. \quad \mathbf{W}_{RF} \in \mathcal{W}_{RF} \end{cases}, \tag{10}$$

where $\mathcal{F}_{RF}, \mathcal{W}_{RF}$ are the feasible set of RF beamformers at the transmitter and receiver side respectively, $\mathbf{F}_{opt}, \mathbf{W}_{MMSE}$ are the unconstrained combiners, $\mathbf{y}$ is the receive signal at the baseband.

On the other hand, [114] proposes to solve the optimization algorithms depicted in (10) using alternating minimization algorithms.

4.1.2.2. Codebook-based precoding

A codebook-based beamforming approach can be applied to the hybrid precoding systems in mmWave. However, in contrast to the analog beamforming approach where only one set of beamfomers have to be optimized, in hybrid precoding we should also design the digital baseband precoders. In case the mutual information is the metric to maximize, the precoder design can be formulated as the solutioin of the following optimization problem,

$$\begin{aligned}(P_3): \quad & \underset{\mathbf{W}_{RF}^H,\mathbf{F}_{RF},\mathbf{F}_{BB}}{\text{maximization}} \quad \log_2 \det\left(\mathbf{I}+\frac{\rho}{\sigma^2}\mathbf{F}_{BB}^H\mathbf{F}_{RF}^H\mathbf{H}\mathbf{W}_{RF}\mathbf{W}_{RF}^H\mathbf{H}\mathbf{F}_{RF}\mathbf{F}_{BB}\right) \\ & s.t. \quad \mathbf{W}_{RF}\in\mathcal{C}_{RF}^{rx} \\ & \qquad \mathbf{F}_{RF}\in\mathcal{C}_{RF}^{tx} \\ & \qquad \mathbf{F}_{BB}\in\mathcal{C}_{BB}^{tx}\end{aligned} \tag{11}$$

where $\mathcal{C}_{BB}^{tx},\mathcal{C}_{RF}^{tx},\mathcal{C}_{RF}^{rx}$ denote the codebooks employed for the digital baseband, RF transmitter and receiver, respectively. The total number of combinations scales exponentially with the dimensions of the different precoders and combineers. In this regard, [115] proposes a reduced complexity precoding taking into account that the mmWave channel is characterized by a few dominant paths, so that the exhaustive search of precoders and combiners is simplified.

4.1.2.3. CAP-MIMO-based precoding

We can combine the analog precoding described in section 4.1.1 with a digital optimization, using the framework of hybrid analog-digital precoding, see Figure 36. The main difference with respect to conventional MIMO is that the transceiver complexity is much simpler.

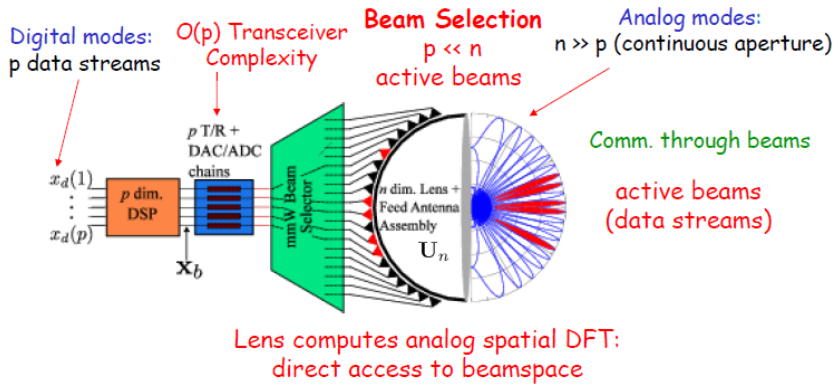

Figure 36: Example of practical Hybrid analog-digital transceiver patented in [116]. Original Figure obtained from [117]

4.1.2.4. Multiuser extensions

The concepts of conventional MIMO multi-user precoding cannot directly apply due to hybrid precoding structure, where RF ($\mathbf{F}_{RF}$) and BB ($\mathbf{F}_{BB}$) beamformers are coupled variables. Moreover the BB beamformer will require the feedback of channel matrices to all users, demanding a large

training and feedback overhead. In [118] it is proposed a two-stage optimization, where first the RF beamformer ($\mathbf{F}_{RF}$) is designed to maximize the received power at each user with a single-user stream, neglecting the interference from other users, so that low training overhead procedures can be used to design the RF beamforming. In the second stage, the base station trains the effective channels, and the *u*-th user feedbacks the equivalent channel $\mathbf{h}_u = \sqrt{\rho}\mathbf{w}_{RF,u}^H \mathbf{H}_u \mathbf{F}_{RF}$. Finally, the BS designs its BB precoder with the obtained quantized channels.

4.1.2.5. Frequency-Selective Fading channel

Most of the works have considered narrow band systems, but how the hybrid precoding has to be extended to a wideband channel is challenging. The solution proposed in [119] considers that the RF beamformer is frequency flat, while the BB beamformer is designed in the frequency domain (i.e. it can apply a different beamformer at each subcarrier). The authors provide the optimal precoding scheme for maximizing the mutual information, and they provide two low-complex precoding algorithms taking into account quantized codebooks and limited feedback.

4.1.3. Low-precision baseband ADCs

At the receiver side, the power consumption can be reduced by using low-precision ADCs, up to one bit with a negligible power consumption that takes into account just the sign of the in-phase and quadrature components of the signals at the output of each RF chain. As it has been reported in section III.C in [108] the ultra-high sampling rate of 240 GSamples per second consumes around 10 mW. Notice that with one bit we are using just the sign of the received signal and useful information to be exploited,

$$\mathbf{z} = \text{sign}(\mathbf{y}) = \text{sign}\left(\sqrt{\rho}\mathbf{W}^H\mathbf{HFs} + \mathbf{W}^H\mathbf{n}\right) \quad (12)$$

However, the fundamentals of the communication constrained to 1-bit quantization differ from the conventional communications [120], and currently capacity characterization is an open research area. In [120] it is shown that low-precision ADCs becomes quasi-optimal in case of working in low to moderate signal-to-noise ratio and small constellations in a large amount of bandwidth. Moreover, the role of channel state information is different and simpler precoding technique, like channel inversion precoding, is much better than the case where the channel has full row rank [121], [122]. Furthermore, the trade-off between the achievable rate and power consumption as a function of the number of bits at the RF chains is investigated in [123].

4.2. Channel Estimation

Working in the mmWave band demands the compensation of the large path loss in the system by means of directional transmissions with very large arrays. Therefore, conventional strategy for MIMO channel estimation considered in lower frequencies, where a pilot signal is transmitted

omnidirectionally, is no longer valid. Notice that the estimated channel is dependent on the analog precoding applied, thus actual channel coefficients cannot be estimated.

It is possible to avoid the explicit channel estimation by using the *codebook beamtraining*, where transmitter and receiver adjust iteratively their beamformers, but this solution limits the implementation of sophisticated transceiver algorithms tackling the multi-user MIMO or interference cancellation. This solution is explored in section 4.2.1. Nevertheless, the channel estimation is simpler in the mmWave band because the channels are sparse in angular and time dimensions. This property allows having good channel estimations from a small set of RF measurements. Different types of techniques are considered in section 4.2.2.

4.2.1. Codebook design for channel estimation under beamtraining

The codebook beamtraining is a conventional procedure where the beam search space (at transmitter and receiver sides) consists of a hierarchical codebook where the best transmit/receive beams are found over the defined codewords. Codewords are grouped in several groups with a different level of angle-precision with the objective of discovering the angular direction of the strongest signal. It has been observed that the search time and detection rate of desired multipath components are highly dependent on the codebook design. In [124] it is proposed a metric named generalized detection probability (GDP) with the objective of evaluating the quality of a given codeword. Using this metric the hierarchical codebook design is proposed which is able to obtain a similar performance than other codebook designs available in the literature, but with fewer RF chains.

This technique can be employed for analog beamforming when the explicit knowledge of channel is not considered. In such a case the beamformers are designed in close-loop beamtraining strategy like in the IEEE 802.11ad. For instance in [125] it is proposed a method where the receiver feeds back a gain and phase value for the dominant RF beams.

4.2.2. Sparse channel estimation for hybrid architectures

Channel estimation at mmWave can be formulated as a sparse problem using ideas based on *adaptive* or *traditional* compressed sensing. Basically, it consists on the following. Let us assume we have M_t beamforming vectors working in M_t time slots. Matrix $\mathbf{X} \in \mathrm{C}^{M_t \times M_t}$ is a diagonal matrix with M_t training symbols on its diagonal, the received signal after M_r measurements is given by,

$$\mathbf{Y} = \sqrt{\rho}\mathbf{W}^H\mathbf{H}\mathbf{F}\mathbf{X} + \mathbf{W}^H\mathbf{n} \tag{13}$$

where $\mathbf{W}, \mathbf{F}$ are defined in (9) as the receive combiners and transmit precoders, respectively.

Assuming that all transmitted symbols are equal, the extended virtual channel model with quantized Angle-of-Arrival (AoA) and Angle-of-Departure (AoD)

$$\mathbf{H} = \mathbf{A}_R \mathbf{H}_b \mathbf{A}_T^*, \quad \mathbf{H}_b = \begin{bmatrix} \alpha_1 & 0 & 0 \\ 0 & \ddots & 0 \\ 0 & 0 & \alpha_{N_p} \end{bmatrix} \tag{14}$$

where $\mathbf{A}_T \in \mathrm{C}^{N_t \times N_p}$ and $\mathbf{A}_R \in \mathrm{C}^{N_r \times N_p}$ denote the array response vectors to the transmitter and receiver respectively, and N_p the number of paths. Assuming that the AoA/AoD are taken from a uniform grid of size G, $\left\{0, 2\pi/G, \ldots, 2\pi(G-1)/G\right\}$, with $G \gg N_p$, then the channel matrix can be approximated by a N_p -sparse matrix $\tilde{\mathbf{H}}_b \in \mathbb{C}^{G \times G}$ with N_p non-zeros elements

$$\mathbf{H} = \bar{\mathbf{A}}_R \tilde{\mathbf{H}}_b \bar{\mathbf{A}}_T^* \tag{15}$$

The received signal using the vectorial (vec) operator is given by

$$\mathrm{vec}(\mathbf{Y}) = \sqrt{\rho}\left(\mathbf{F}^T \bar{\mathbf{A}}_T^* \otimes \mathbf{W}^H \bar{\mathbf{A}}_R^*\right)\mathrm{vec}\left(\tilde{\mathbf{H}}_b\right) + \mathrm{vec}\left(\mathbf{W}^H \mathbf{n}\right) \tag{16}$$

where symbol $\otimes$ denotes the kronecker product.

The channel estimation can be formulated as a non-convex combinatorial problem

$$\begin{aligned} (P_4): \quad & \underset{\mathbf{h}_b}{\text{minimize}} \quad \|\mathbf{h}_b\|_0 \\ & s.t. \quad \left\|\mathrm{vec}(\mathbf{Y}) - \sqrt{\rho}\left(\mathbf{F}^T \bar{\mathbf{A}}_T^* \otimes \mathbf{W}^H \bar{\mathbf{A}}_R^*\right)\mathbf{h}_b\right\| \le \sigma \end{aligned} \tag{17}$$

with $\mathbf{h}_b = \mathrm{vec}\left(\tilde{\mathbf{H}}_b\right)$

4.2.2.1. Channel estimation with low-precision ADCs

Having one-bit ADCs at receiver side simplifies the estimation used with the framework introduced in [122]

$$\begin{aligned} (P_5): \quad & \underset{\mathbf{h}_b}{\text{minimize}} \quad \|\mathbf{h}_b\|_0 \\ & s.t. \quad \left\|\mathrm{sign}\left(\mathrm{vec}(\mathbf{Y})\right) - \sqrt{\rho}\,\mathrm{sign}\left(\left(\mathbf{F}^T \bar{\mathbf{A}}_T^* \otimes \mathbf{W}^H \bar{\mathbf{A}}_R^*\right)\mathbf{h}_b\right)\right\| \le \sigma \end{aligned} \tag{18}$$

The optimization can be solved using the generalized approximate message passing (GAMP) algorithm in a few iterations.

Recent results presented in [126] show that in large MIMO systems with low-precision ADCs, not necessarily in the mmWave band, the joint estimation of channel and data improves significantly the results obtained with pilot-only estimation.

4.2.2.2. Multi-user channel estimation

Channel estimation in a multi-user mmWave system is investigated in [127] where a low-complexity method based on compressed sensing channel estimation and conjugate analog beamforming is proposed. In addition to require small training overhead with respect the channel matrix dimensions

it can be elucidated the number of measurements needed to maximize the effective sum-rate of the system.

4.2.2.3. Frequency-Selective Fading channel

In general, the channel estimation algorithms proposed in the literature assume a narrow-band flat fading channel, but mmWave tend to have frequency-selective fading (FSF) due to the large bandwidth and the different delays of multipath. In [128] it is proposed a multi-user uplink channel estimation where the broadband FSF is decomposed into multiple narrow-band flat fading channels by means of the OFDM. A distributed compressive sensing-based channel estimation is carried out, seizing the sparsity of the angle-domain in order to reduce the training overhead.

4.3. Research roadmap

The research topics addresed in 5GWireless will follow two main directions:

- *Investigate the optimal precoder design and channel estimation with low-precision ADCs*. How the results in the state-of-the-art can be extended to the multi-user case and/or to frequency selective fading channels is a promising area to be considered. This approach allows an important reduction in terms of complexity.

- *Benefits of channel sparsity in precoding and channel estimation in the hybrid-precoding approach*. Continue investigating how precoders and channel estimation procedures can make good use of the properties of the channel in the mmWave band for the multi-user case and frequency selective channels.

In all cases, the research will be done from the signal processing point of view, i.e. providing tools, algorithms, or fundamental bounds of the different topics investigated in the mmWave.

5. MmWave-based cellular networking

One of the objectives for 5G is to propose 10 to 100 times higher data rate to mobile users, which is in the order of 10 Gbps. MmWave communications are a key enabler for this objective thanks to abundant and contiguous bandwidth resources. In addition, the antenna small size allows for large antenna arrays in a small form factor, allowing high directivity with beamforming, low interference and high spatial reuse. The spectrum resources should be shared between the access network (towards users) and the wireless backhaul [129] [130].

5G could thus rely on a mmWave-based last mile network with ultra-dense node deployments, i.e. few meter Inter-Site Distance (ISD) indoors and between 50 m and 200 m outdoors. The dense deployment of infrastructure nodes will make traditional wire-based or point-to-point backhaul provisioning challenging. Wireless self-backhauling from point-to-multipoint hubs (in sub-6GHz band) or over multiple hops (possibly in mmWave band) is proposed to enhance flexibility and facilitate dense deployments [131].

Ultra-dense networks will by the way introduce other challenges, such as the mobility management. To avoid frequent handover procedures, it is proposed to separate the control and data planes [132]. The control channels would be provided by macro eNB operating in the microwave band, while high data rate services would be supported simultaneously by small-cells in the mmWave band.

An interesting overview on the challenges related to mmWave-based access networks is given in [133]. As the mmWave small-cells show a radius between 100 and 200 meters in dense urban areas (as deduced from initial outdoor measurements), the required outdoor small-cell topologies are not expected to be very different from the ones that are envisaged in traditional cellular frequency bands. Of course, the small-cell locations must be chosen such that LOS links are maximized. Besides, the coverage and access procedures will face new difficulties due to the strong propagation and shadowing losses:

- Strong path-loss can be compensated by highly directional transmissions, but the signal is severely vulnerable to shadowing, which results in **outages and intermittent signal quality**. Consequently, the communication network must be able to adapt to fast degrading channel quality, either from rapid handover to a neighbour small-cell or to the macro network layout that operates in the microwave band, or from adaptative beamforming. This requires efficient and appropriate channel sensing techniques, which are made more complex by the necessary directive transmissions. One solution, which is also relevant to support high density small-cell handover procedures, may be to simultaneously attach the user to several cells. In any case, the communication protocol must be able to support intermittent transmissions.
- Since directive transmission is required between the base station and the user, **new cell search and access procedures** have to be defined. Detection of the synchronization and broadcast signals used in the initial cell search needs an angle scan to be performed. The handover and the random access procedures will be delayed due to this necessary beam alignment. This issue is addressed in details in [134], were a random access methodology (Figure 37) and adapted frame structure are proposed (Figure 38). The RACH (Random

Access Channel) frame is extended to multiple preambles, i.e. consecutive slots composed of the cyclic prefix (RCP), preamble sequence and guard time (GT), but with different transmit beams. The base station receive the signals using different receive beams, such that all Tx/Rx beam alignments can be mapped.

- As directive transmission and strong propagation and shadowing losses dramatically reduce the interference levels, the interference mitigation techniques that have been elaborated for lower-frequency dense networks, like inter-cell interference cancellation or multi-cell cooperation, are expected to have only limited impact in mmWave band.
- **Relaying** may be at the heart of future mmWave small-cell topologies, by facilitating backhaul deployments, extending the outdoor coverage (from device-to-device multi-hops), or extending the coverage to inside the buildings and vehicles. This is viewed as a low-cost alternative to the deployment of even higher density of antennas.
- The **channel sensing and feedback quantization** must be adapted to the specificities of the mmWave channel, meaning that the coherence time is shorter than at traditional frequencies, that the multi-path channel is more sparse, and that sensing must be directive.

  A compromise or appropriate combining must be found between **TDMA scheduling** (i.e. one user per time slot), which is compliant with practical low-power MIMO or beamforming processing along with large number of antenna elements, and **FDMA multiplexing** (distribution of frequency slots to different simultaneous users), which permits to efficiently support small-packet transmissions and offers a solution for power-limited user equipments that will allocate and process only a portion of the wide available bandwidth.

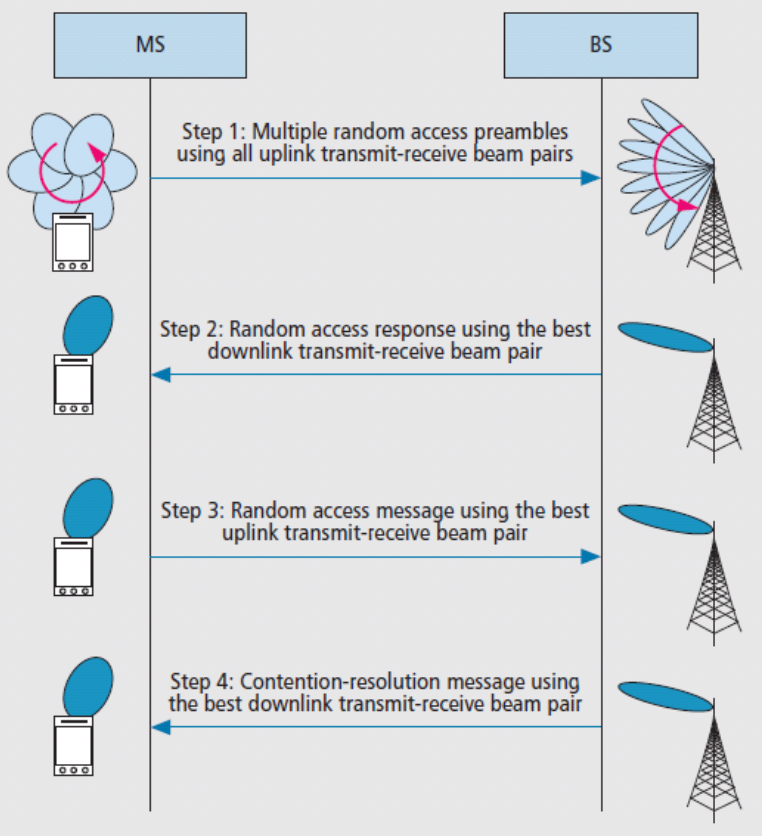

Figure 37. Proposed random access procedure in [134]

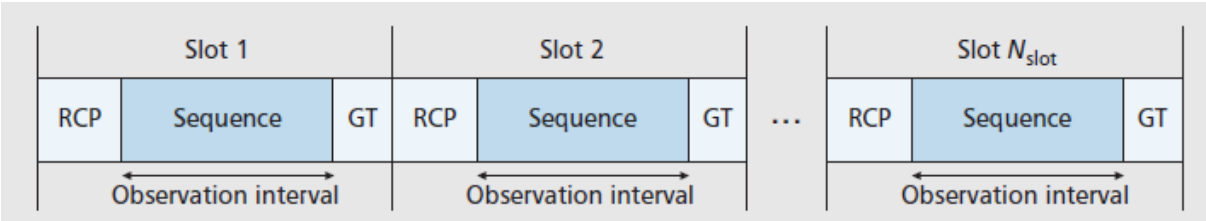

Figure 38. Example of frame structure proposed in [134].

Recent studies have compared the capacity of traditional LTE small-cell networks to the one that is expected with mmWave technologies. For instance, [135] uses a stochastic approach to model random blockages due to buildings, evaluates different beamforming strategies, including multi-user beamforming, and predicts the propagation from a stochastic cluster-based channel model. The system simulation at frequency 28 GHz with 100 MHz bandwidth and a cell radius of 100 meters is compared to the simulation of a microwave network with bandwidth 20 MHz and cell radius 200 meters. Finally, SU-beamforming at mmWave provides an average cell throughput 5.8 times higher than microwave SU-MIMO. The MU-beamforming leads to twice this throughput. The capacity analysis in [133] considers a mmWave system with 1 GHz bandwidth at 28 GHz and 73 GHz, and relies on the urban small-cell scenario defined by 3GPP. The cell radius is 100 meters. The propagation is predicted from channel model derived from the New-York city measurements presented in section 2.2.2. Results are shown in Figure 39. Compared to a traditional LTE network with same small-cell density, the DL network capacity is multiplied by 26 and 20 at respectively 28 GHz and 73 GHz.

System	BW & Duplex	BS antenna	UE antenna	fc (GHz)	Spec. eff (bps/Hz)		Cell capacity (Mbps)		5% Cell edge rate (Mbps)	
					DL	UL	DL	UL	DL	UL
mmW	1 GHz TDD	8x8	4x4	28	2.25	2.38	1130	1190	17.4	21.6
		8x8	8x8	28	2.83	2.84	1420	1420	32.7	36.3
		8x8	4x4	73	1.45	1.65	730	830	6.6	9.6
		8x8	8x8	73	2.15	2.31	1080	1160	16.6	22.1
LTE	20+20 MHz FDD	2 TX, 4 RX	2	2.5	2.69	2.36	53.8	47.2	1.80	1.94

Note 1. Assumes 20% overhead and 50% UL-DL duty cycle for the mmW system
Note 2. Long-term, non-coherent beamforming are assumed at both the BS and UE in the mmW system. However, the mmW results assume no spatial multiplexing gains, whereas the LTE results from [83] include spatial multiplexing and beamforming.

Figure 39. Comparison of capacities in small-cell deployments relying respectively on a traditional LTE network and expected mmWave network [133]

Finally, we describe here below different deployment scenarios that are imagined in the literature to involve mmWave links. Those could inspire the scenarios considered in the 5Gwireless project to drive and organize the investigations. First, Figure 40 from [136] illustrates five scenarios where mmWave communications are employed for different types of link:

- Scenario 1 = baseline: Macro and small-cells are operated in microwave bands, and are backhauled with optical fiber.
- Scenario 2: The communications of users connected to small-cells are using mmWave band.

- Scenario 3: The small-cells are connected to the donor macro-cell by single-hop mmWave backhaul, while the access network only relies on microwave technology.
- Scenario 4: Both the small-cell backhaul and access are using mmWave band.
- Scenario 5: Multi-hop backhaul facilitates the deployment and connection of small-cells.

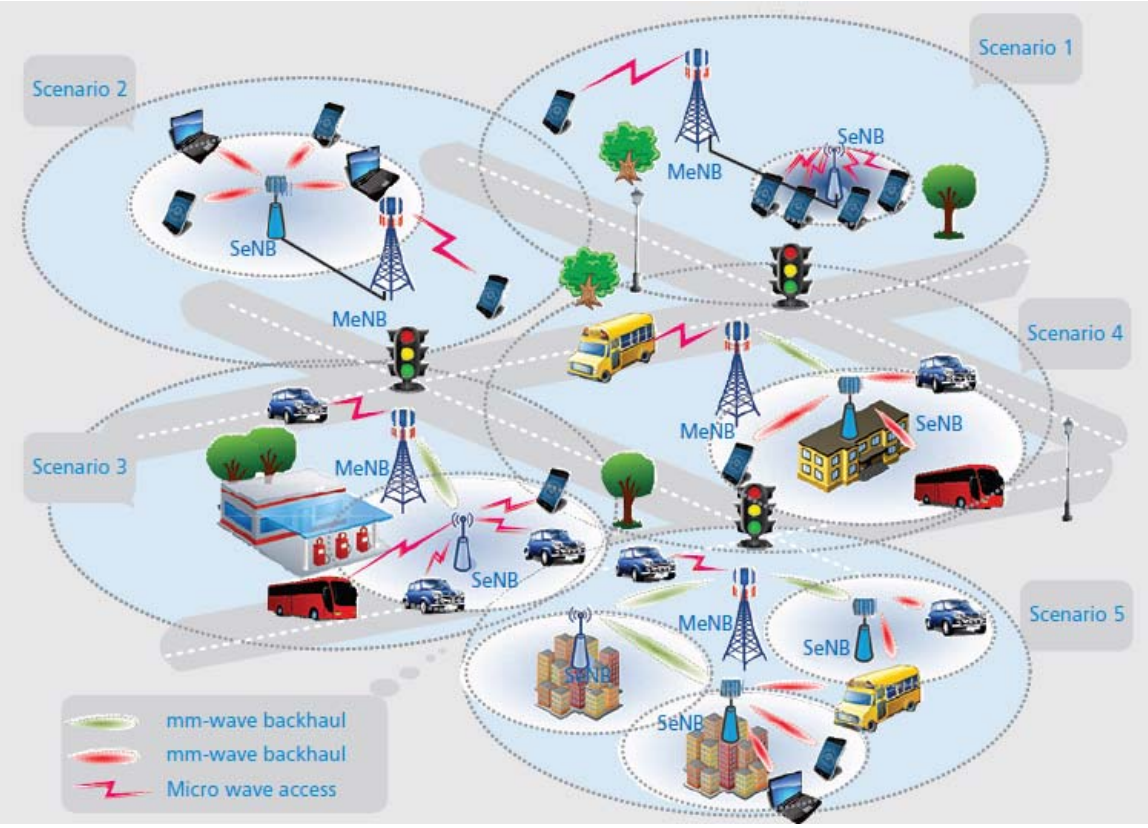

Figure 40. Proposed network architecture scenarios in [136]

The paper [137] presents possible deployment cases in a quite different way, more focusing on the type of environment and capacity targets. This actually is a summary of the scenarios defined in the MiWEBA project:

- Indoor scenarios:
  - Isolated rooms: this scenario can apply to provide high capacity in an exhibition hall or an open-space office environment, covered by several mmWave nano-cells; cooperative transmission can be implemented; the mobility within the room can be facilitated if control-plane and data-place are separated.
  - Large public areas: this scenario covers hotspot areas composed of multiple rooms like typical malls, shopping centers, airports, etc.
- Outdoor scenarios:
  - Hotspots: in this scenario, the mmWave small-cells are deployed in isolated areas where the data rate offered by existing LTE/LTE-A deployments is not sufficient.
  - High-rate areas: the combination of the traditional macro network at microwave frequency and a small number of mmWave small-cells provide almost full coverage in the area; inter-cell interference is limited and can manged with simple cooperation and alignment techniques; improved handover is needed to support the

user mobility, e.g. using separation between data plane and control plane, or context management.

- Larger areas and denser deployment: similar to the previous scenario, this one involves a huge number of mmWave small-cells. Higher inter-cell cooperation is required to mitigate interference, while the high small-cell density combined with joint transmission (coordinated downlink transmission from several base stations to a single end user) allows for an even increased spectral efficiency. Dynamic creation of virtual cells is another technique that would permit to optimize the network wireless access according to the user demand.

6. Conclusion

The 5Gwireless D2.1 deliverable first presents all the benefits that are expected from the introduction of mmWave frequency bands in the access of future mobile communication networks: new frequency resources and large reachable data rates. Progress in mmWave electronic components and antennas was driven in last years by the emergence of 60 GHz WLAN systems and finally makes the mobile mmWave communications one of the key promising features in the 5G technology portfolio. The counterpart relies in strong path-loss and shadowing loss. This can be overcome by the employment of high-gain directive antennas and dense small-cell deployments.

The deliverable describes the technical challenges, state-of-the-art and research perspective on mmWave beamforming antenna techniques and related signal processing.

It also reviews the current work and limitations on mmWave propagation measurements, stochastic channel modelling and deterministic approaches, in particular ray-based models. The major trend in mmWave antenna seems to be the elaboration of very large antenna arrays along with hybrid digital/analogue beamforming, which is the result of a trade-off between the complexity (or cost), power consumption and flexibility.

Finally, the document ends with an overview on the mmWave-devoted networking strategies, which combine high cell densification, beamforming, network heterogeneity, relaying techniques, and specific access procedures. Some scenarios defined in literature are also identified that could be source of inspiration in later 5Gwireles studies.

Deliverable D2.1 is thought to pave the way towards relevant and promising research activity within the 5Gwireless project, including channel measurements, channel modelling enhancements and validation, investigation and prototyping on new beamforming antennas and signal processing, as well as appropriate mmWave network deployment (access and last mile backhaul).

References

[1] ITU-R P.676-10, *Attenuation by atmospheric gases*, 2013.

[2] H. Mehrpouyan, M. Matthaiou, R. Wang, G.K. Karagiannidis& Y. Hua, "Hybrid Millimeter-Wave Systems: A Novel Paradigm for HetNets", *IEEE communication magazine*, Jan. 2015.

[3] ITU-R P.837-2, *Characteristics of precipitation for propagation modelling*, 1999.

[4] ITU-R P.1238-7, *Propagation data and prediction methods for the planning of indoor radiocommunication systems and radio local area networks in the frequency range 900 MHz to 100 GHz*, 2012.

[5] S.R. Saunders, *Antenna and propagation for wireless communication systems*, Wiley &sons, 1999.

[6] M. K. Samimi, T. S. Rappaport, and G. R. MacCartney, "Probabilistic omnidirectional path loss models for millimeter-wave outdoor communications", *IEEE Communications Letters*, 2015.

[7] E. J. Violette, R. H. Espeland, & F. Schwering, "Vegetation Loss Measurements at 9.6, 28.8, and 57.6 GHz through a Pecan Orchard in Texas",Army communications – Electronics command Fort Monmouth NJ, 1983.

[8] I. Rodriguez, R. Abreu, E. P.L. Almeida, M. Lauridsen, A. Loureiro& P. Mogensen, "24 GHz cmWave Radio Propagation Through Vegetation: Suburban Tree Clutter Attenuation", 10th Conference on Antennas and Propagation (EuCAP 2016), Davos, Switzerland, 2016.

[9] ITU-R P.833-7,*Attenuation in vegetation*, 2012.

[10] S. Collonge, G. Zaharia, and G. E. Zein, "Influence of the human activity on wide-band characteristics of the 60 GHz indoor radio channel", *IEEE Transactions on Wireless Communications*, 2004.

[11] R. J. Weiler, W. Keusgen, A. Maltsev, T. Kühne, A. Pudevey, L. Xian, J. Kim and M. Peter, "Millimeter-Wave Outdoor Access Shadowing Mitigation Using Beamforming Arrays", 10th Conference on Antennas and Propagation (EuCAP 2016), Davos, Switzerland, 2016.

[12] T. S. Rappaport, G. R. MacCartney, M. K. Samini, and S. Sun, "Wideband Millimeter-Wave Propagation Measurements and Channel Models for Future Wireless Communication System Design", *IEEE Transactions on Communications*, vol. 63, no. 9, Sept. 2015.

[13] 3GPP, TR 36.873 (V12.2.0), *Study on 3D channel model for LTE*, July 2015.

[14] 5GCM White Paper, *5G Channel Model for bands up to 100 GHz*, version 2.0, March 2016.

[15] G. R. MacCartney, T. S. Rappaport, M. K. Samini, and S. Sun, "Millimeter-Wave Omnidirectional Path Loss Data for Small Cell 5G Channel Modeling", *IEEE Access*, 2015

[16] S. Shu et al., "Investigation of Prediction Accuracy, Sensitivity, and Parameter Stability of Large-Scale Propagation Path Loss Models for 5G Wireless Communications", in *IEEE Transactions on Vehicular Technology*, 2016.

[17] M. Peter, et al., *Measurement campaigns and initial channel models for preferred suitable frequency ranges*, mmMAGIC Deliverable D2.1, March 2016.

[18] H. Zhao et al., "28 GHz millimeter wave cellular communication measurements for reflection and penetration loss in and around buildings in New York city", in 2013 IEEE International Conference on Communications (ICC), pp. 5163-5167, 9-13 June 2013.

[19] C. Larsson, F. Harrysson, B-E. Olssson, and J-E. Berg, "An outdoor-to-indoor propagation scenario at 28 GHz", in *Proc. of European Conference on Antennas and Propagation (EuCAP) 2014*, pp. 3301-3304, 2014.

[20] Y. Lostanlen, Y. Corre, Y. Louet, Y. Le Helloco, S. Collonge and G. El-Zein, "Comparison of measurements and simulations in indoor environments for wireless local networks at 60 GHz", in Proceedings of IEEE 55th Vehicular Technology Conference (VTC Spring 2002), 2002.

[21] W. Fan, I. Carton and G. F. Pedersen, "Comparative Study of Centimetric and Millimetric Propagation Channels in Indoor Environments", 10th Conference on Antennas and Propagation (EuCAP 2016), Davos, Switzerland, 2016.

[22] S. Salous and Y. Gao, "Wideband Measurements in Indoor and Outdoor Environments in the 30 GHz and 60 GHz Bands", 10th Conference on Antennas and Propagation (EuCAP 2016), Davos, Switzerland, 2016.

[23] T. S. Rappaport, S. Sun, R.Mayzusand H. Zhao, "Millimeter Wave Mobile Communications for 5G Cellular: It Will Work!",*IEEE Access*, 2013.

[24] M. K. Samimi and T. S. Rappaport,"Local Multipath Model Parameters for Generating 5G Millimeter-Wave 3GPP-like Channel Impulse Response", 10th Conference on Antennas and Propagation (EuCAP 2016), Davos, Switzerland, 2016.

[25] B. Peng and T. Kürner, "Channel Characteristics Study for Future Indoor MillimeterAndSubmillimeter Wireless Communications", 10th Conference on Antennas and Propagation (EuCAP 2016), Davos, Switzerland, 2016.

[26] M. K. Samimi, T. S. Rappaport, "3-D statistical channel model for millimeter-wave outdoor mobile broadband communications," in *2015 IEEE International Conference on in Communications (ICC)*, pp.2430-2436, 8-12 June 2015.

[27] L. Raschkowski, et al., *METIS channel models*, METIS Deliverable D1.4, Feb. 2015.

[28] A. Saleh and R. Valenzuela, "A Statistical Model for Indoor Multipath Propagation," IEEE JSAC, Feb. 1987.

[29] 3GPP TR25.996 v13.0.0, *Spatial channel model for multiple input multiple output (MIMO) simulations*, 2015.

[30] P. Kyösti, et al., *WINNER II Channel Models*, IST-WINNER II Deliverable 1.1.2 v.1.2, Feb. 2008.

[31] P. Heino, et al.,*WINNER+ Final Channel Models*, WINNER+ Deliverable D5.3 V1.0, Jun. 2010.

[32] A. Ghazal, C.-X. Wang, B. Ai, D. Yuan, and H. Haas, "A non-stationary wideband MIMO channel model for high-mobility intelligent transportation systems," *IEEE Trans. Intell. Transp. Syst.*, vol. 16, no. 2, pp. 885-897, Apr. 2015.

[33] S. Wu, C.-X. Wang, H. Haas, H. Aggoune, M. M. Alwakeel, and B. Ai, "A non-stationary wideband channel model for massive MIMO communication systems," *IEEE Trans. Wireless Commun.*, vol. 14, no. 3, pp. 1434-1446, Mar. 2015.

[34] X. Cheng, C.-X. Wang, B. Ai, and H. Aggoune, "Envelope level crossing rate and average fade duration of non-isotropic vehicle-to-vehicle Ricean fading channels", *IEEE Trans. Intell. Transp. Syst.*, vol. 15, no. 1, pp. 62-72, Feb. 2014.

[35] Y. Yuan, C.-X. Wang, X. Cheng, B. Ai, and D. I. Laurenson, "Novel 3D geometry-based stochastic models for non-isotropic MIMO vehicle-to-vehicle channels", *IEEE Trans. Wireless Commun.*, vol. 13, no. 1, pp. 298-309, Jan. 2014.

[36] X. Cheng, C.-X. Wang, H. Wang, X. Gao, X.-H. You, D. Yuan, B. Ai, Q. Huo, L. Song, and B. Jiao, "Cooperative MIMO channel modeling and multi-link spatial correlation properties," *IEEE J. Sel. Areas Commun*., vol. 30, no. 2, pp. 388-396, Feb. 2012.

[37] H. C. Nguyen, H. Cong, et al., "Evaluation of empirical ray-tracing model for an urban outdoor scenario at 73 GHz E-Band", 80th IEEE Vehicular Technology Conference (VTC Fall), 2014.

[38] S. Baek, Y. Chang, H. Kim, and A.Agiwal, "Comparison Analysis of Outdoor Channel Characteristics at 28 GHz and 2 GHz Using 3D Ray-Tracing Technique", 80th IEEE Vehicular Technology Conference (VTC Fall), 2014.

[39] N. F. Abdullah, et al., "Channel Parameters and Throughput Predictions for mmWave and LTE-A Networks in Urban Environments", 81st IEEE Vehicular Technology Conference (VTC Spring), 2015.

[40] Z. Zhang, et al., "Coverage and channel characteristics of millimeter wave band using ray tracing",IEEE International Conference on Communications (ICC), 2015.

[41] T. A. Thomas, et al., "3D mmWave channel model proposal", 80th IEEE Vehicular Technology Conference (VTC Fall), 2014.

[42] S. Hur, S. Baek, B. Kim, J. Park, A. F. Molisch, K. Haneda, and M. Peter, "28 GHz channel modeling using 3D ray-tracing in urban environments", EUCAP 2015, April 2015.

[43] Q. Li, et al., "Validation of a Geometry-Based Statistical mmWave Channel Model Using Ray-Tracing Simulation", 81st IEEE Vehicular Technology Conference (VTC Spring), 2015.

[44] S. Baek, et al., "3-Dimensional Large-Scale Channel Model for Urban Environments in mmWave Frequency", IEEE International Conference on Communication Workshop (ICCW), 2015.

[45] ITU-R Rec. P.1410-5, *Propagation data and prediction methods required for the design of terrestrial broadband radio access systems operating in a frequency range from 3 to 60 GHz*, 2012.

[46] N. J. Thomas, M. J. Willis and K. H. Craig "Analysis of the dominant propagation mechanisms for radio coverage and interference prediction in urban scenarios at 2.4, 5.8 & 28.0 GHz", 10th Conference on Antennas and Propagation (EuCAP 2016), Davos, Switzerland, 2016.

[47] Y. Corre, T. Tenoux, J. Stéphan, F. Letourneux and Y. Lostanlen, "Analysis of Outdoor Propagation and Multi-Cell Coverage from Ray-Based Simulations in sub-6GHz and mmWave Bands", 10th Conference on Antennas and Propagation (EuCAP 2016), Davos, Switzerland, 2016.

[48] C. Dehos, J. Gonzalez, A. De, D. Kténas and L. Dussopt "Millimeter-wave access and backhauling: the solution to the exponential data traffic increase in 5G mobile communications systems?", *IEEE Communication Magazine*, vol. 52, no. 9, pp.88 -95, Sept. 2014.

[49] Y. Corre and Y. Lostanlen, “Three-Dimensional Urban EM Wave Propagation Model for Radio Network Planning and Optimization Over Large Areas”,*IEEE Transactions on Vehicular Technology*, vol. 58, no. 7, pp. 3112–3123, Sep. 2009.

[50] MiWEBA, *Channel modeling and characterization*, MiWEBA Deliverable D5.1, Jun. 2014.

[51] A.-F. Molisch, Wireless Communications, *John Wiley & Sons,* West Sussex, UK, 1st edition, 2006.

[52] C. Gustafson, K. Haneda, S. Wyne and F. Tufvesson, "On mm-Wave Multipath Clustering and Channel Modeling," *IEEE Transactions on Antennas and Propagation*, vol. 62, no. 3, pp. 1445-1455, March 2014.

[53] R. Muller et al., "Ultra-Wideband Channel Sounder for Measurements at 70 GHz," in IEEE 81st Vehicular Technology Conference (VTC Spring), Glasgow, 2015.

[54] R. Müller, D. A. Dupleich, C. Schneider, R. Herrmann and R. S. Thomä, "Ultrawideband 3D mmWave channel sounding for 5G," in XXXIth URSI General Assembly and Scientific Symposium Beijing, 2014.

[55] R. J. Weiler, M. Peter, T. Kühne, M. Wisotzki and W. Keusgen, "Simultaneous millimeter-wave multi-band channel sounding in an urban access scenario," in 2015 9th European Conference on Antennas and Propagation (EuCAP), Lisbon, 2015.

[56] H.-K. Kwon, M.-D. Kim, and Y.-J. Chong, “Implementation and performance evaluation of mmWave channel sounding system,” in *IEEE International Symposium on Antennas and Propagation & USNC/URSI National Radio Science Meeting*, 2015.

[57] A. L. Swindlehurst, E. Ayanoglu, P. Heydari and F. Capolino, “Millimeter-wave massive MIMO: the next wireless revolution?,” *IEEE Communications Magazine*, vol. 52, no. 9, pp. 56-62, September 2014.

[58] Z. Wen and H. Kong, "mmWave MIMO channel sounding for 5G," in *5G for Ubiquitous Connectivity (5GU)*, 2014 1st International Conference on, Akaslompolo, pp. 192-197, 2014.

[59] H. Wang and M. Kaveh, “Coherent signal-subspace processing for the detection and estimation of angles of arrival of multiple wideband sources,” *IEEE Trans. Acoust., Speech, Signal Process.*, vol. ASSP-33, no. 4, pp. 823–831, Aug. 1985.

[60] A. F. Molisch “Ultra-Wide-Band Propagation Channels”, *Proceedings of the IEEE*, 2009.

[61] W. Li, W. Yao, and P.J. Duffett-Smith, “Comparative study of joint TOA/DOA estimation techniques for mobile positioning applications”, in *Proceedings of the 6th IEEE Conference on Consumer Communications and Networking Conference*, 2009.

[62] G. R. MacCartney, Jr., T. S. Rappaport, S. Sun, and S. Deng, “Indoor office wideband millimeter-wave propagation measurements and channel models at 28 GHz and 73 GHz for ultra-dense 5G wireless networks (Invited),” *IEEE Access,* vol. 3, pp. 2388-2424, Dec. 2015.

[63] S. Sun et al., “Investigation of prediction accuracy, sensitivity, and parameter stability of large-scale propagation path loss models for 5G wireless communications,” *IEEE Transactions on Vehicular Technology*, vol. 65, no. 5, pp. 1-18, May 2016.

[64] S. Sun, G. R. MacCartney, Jr., and T. S. Rappaport, “Millimeter-Wave Distance-Dependent Large-Scale Propagation Measurements and Path Loss Models for Outdoor and Indoor 5G Systems,” in the 10th European Conference on Antennas and Propagation (EuCAP 2016), April 2016.

[65] M. K. Samimi, T. S. Rappaport, “Statistical Channel Model with Multi-Frequency and Arbitrary Antenna Beamwidth for Millimeter-WaveOutdoor Communications,” in 2015 IEEE Global Communications Conference, Exhibition & Industry Forum (GLOBECOM) Workshop, Dec. 6-10, 2015.

[66] M. K. Samimi, T. S. Rappaport, “Ultra-wideband statistical channelmodel for non line of sight millimeter-wave urban channels,” in 2014 IEEE Global Communications Conference (GLOBECOM), pp. 3483-3489, 8-12Dec. 2014.

[67] M. Samimi et al., “28 GHz Angle of Arrival and Angle of Departure Analysis for Outdoor Cellular Communications Using Steerable Beam Antennas in New York City,” in 2013 IEEE Vehicular Technology Conference (VTC Spring), pp.1-6, 2-5 June 2013.

[68] W. Roh and J. Y. Seol and J. Park and B. Lee and J. Lee and Y. Kim and J. Cho and K. Cheun and F. Aryanfar, "Millimeter-wave beamforming as an enabling technology for 5G cellular communications: theoretical feasibility and prototype results," *IEEE Communications Magazine*, vol. 52, no. 2, pp. 106-113, February 2014.

[69] A. Molisch, F. Tufvesson, “Propagation channel models for next-generation wireless communications systems,” *IEICE Transactions on Communications*, Vol. E97B, No. 10, pp. 2022-2034, 2014.

[70] T. Bai, V. Desai and R. W. Heath, "Millimeter wave cellular channel models for system evaluation," in 2014 International Conference on Computing, Networking and Communications (ICNC), pp. 178-182, Honolulu, HI 2014.

[71] J. Lee, Y. Song, E. Choi and J. Park, "mmWave cellular mobile communication for Giga Korea 5G project," in 2015 21st Asia-Pacific Conference on Communications (APCC), pp. 179-183, Kyoto, Japan, 2015.

[72] T. Mavridis, L. Petrillo, J. Sarrazin, D. Lautru, A. Benlarbi-Delai and P. De Doncker, "Theoretical and Experimental Investigation of a 60-GHz Off-Body Propagation Model," *IEEE Transactions on Antennas and Propagation*, vol. 62, no. 1, pp. 393-402, Jan. 2014.

[73] L. Wei, R. Q. Hu, Y. Qian and G. Wu, "Key elements to enable millimeter wave communications for 5G wireless systems," *IEEE Wireless Communications*, vol. 21, no. 6, pp. 136-143, December 2014.

[74] Q. Li, H. Shirani-Mehr, T. Balercia, H. Niu, A. Papathanassiou and G. Wu, "Millimeter wave channel model and system design considerations," in 2015 IEEE International Conference on Communication Workshop (ICCW) , pp. 1214-1219, London, 2015.

[75] Q. C. Li, G. Wu and T. S. Rappaport, "Channel model for millimeter-wave communications based on geometry statistics," in Globecom Workshops (GC Wkshps), pp. 427-432, Austin, TX, 2014.

[76] Y. Wang, L. Huang, Z. Shi, K. Liu, and X. Zou, “A millimeter wave channel model with variant angles under 3GPP SCM framework,” in 26th Annual International Symposium on Personal, Indoor, and Mobile Radio Communications (PIMRC), 2015.

[77] X. Wu, Y. Zhang, C.-X. Wang, G. Goussetis, H. Aggoune, and M. M. Alwakeel, “28 GHz indoor channel measurements and modelling in laboratory environment using directional antennas”, invited paper, in *Proc. EuCAP’15*, Lisbon, Portugal, Apr. 2015.

[78] S. Anderson, M. Millnert, M. Viberg,”An adaptive array for mobile communication systems”, *IEEE transactionson Vehicular technology*, Vol 40, No 2, 1991.

[79] V. Basavarajappa, *Design of a wideband conformal array antenna system with beamforming and null steering, for application in a DVB-T based passive radar*, Thesis, 2012.

[80] W. Liu, S. Weiss, *Wideband beamforming concepts and techniques*, Wiley series, 2010.

[81] D.Liu, U.Pfeiffer, J.Grzyb, and B. Gauche,*Advancedmillimeter-wave technologies: antennas, packaging and circuits*,John Wiley&Sons, 2009.

[82] S. Kutty, and D. Sen, *Beamforming for Millimeter Wave Communications: An Inclusive Survey*, 2015.

[83] J. Li, L. Xiao, X. Xu, and S. Zhou, "Robust and Low Complexity Hybrid Beamforming for Uplink Multiuser MmWave MIMO Systems”, in *IEEE Communications Letters*, 2016.

[84] T. S. Rappaport, G. R. Mac Cartney, M. K. Samimi, and S. Sun, “Wideband millimeter-wave propagation measurements and channel models for future wireless communication system design,” *IEEE Trans. Commun.*, vol. 63, no. 9, pp. 3029-3056, Sep. 2015.

[85] X. Gao, L. Dai, C. Yuen, and Z. Wang, “Turbo-Like Beamforming Based on Tabu Search Algorithm for Millimeter-Wave Massive MIMO Systems”, in *IEEE Transactions on Vehicular Technology*, 2015.

[86] F. Bøhagen, P. Orten, and G. E. Øien, “Design of optimal highrank line-of-sight MIMO channels,” *IEEE Transactions on Wireless Communications*, vol. 6, no. 4, pp. 1420–1424, 2007.

[87] N. Ishikawa, R. Rajashekar, S. Sugiura, and L. Hanzo, “Generalized Spatial Modulation Based Reduced-RF-ChainM illimeter-Wave Communications”, in *IEEE Transactions on Vehicular Technology* , 2016.

[88] Y. Kim, H-Y Lee, P. Hwang, R-K Patro, J. Lee, W. Roh, and K. Cheun, “Feasibility of Mobile Cellular Communications at Millimeter Wave Frequency”, in *IEEE Journal of Selected Topics in Signal Processing*, 2016.

[89] K. Zheng, L. Zhao, J. Mei, B. Shao, W. Xiang, and L. Hanzo, “Survey of Large-Scale MIMO Systems", *IEEE Communications Surveys & Tutorials*, vol. 17, no. 3, pp. 1738-1760, 2015.

[90] L. Lu, G.Y. Li, A.L. Swindlehurst, A. Ashikhmin, and R. Zhang, “An Overview of Massive MIMO: Benefits and Challenges”, *IEEE Journal of Selected Topics in Signal Processing*, vol. 8, no. 5, pp. 742-758, 2014.

[91] R. Mendez-Rial, C.Rusu, N. Gonzalez-Prelcic, A.Alkhateeb, and R. W. Heath, “Hybrid MIMO Architectures for Millimeter Wave Communications: Phase Shifters or Switches?”, *IEEE Access*, 2016.

[92] J-S Park, J-B Ko, H-K Kwon, B-S Kang, B. Park, and D. Kim, “A tilted combined beam antenna for 5G communications using a 28 GHz band”, in *IEEE Antennas and Wireless Propagation Letters*, 2016.

[93] M. Runbo, G.Yue, C.Parini, L. Cuthbert, “Dual-polarized turning torso antenna array for massive MIMO systems”, in 9th European Conference on Antennas and Propagation (EuCAP 2015), April 2015.

[94] Y. Luo, Q-X Chu, D-L Wen, “A ±45° Dual-Polarized Base-Station Antenna with Enhanced Cross-Polarization Discrimination via Addition of Four Parasitic Elements Placed in a Square Contour”, in *IEEE Transactions on Antennas and Propagation*, 2016.

[95] S. Beer, T. Zwick, “122 GHz antenna-integration in a plastic package based on a flip chip interconnect”, in Microwave Workshop Series on Millimeter Wave Integration Technologies (IMWS), 2011 IEEE MTT-S International , pp.37-40, 15-16 Sept. 2011.

[96] V. Miraftab, Z. Wenyao, M. Repeta, “A wideband low cost E-band SIW antenna array for high capacity mmWave radio”, in Microwave Symposium (IMS), 2015 IEEE MTT-S International , pp.1-3, 17-22 May 2015.

[97] B.K. Tehrani, B.S. Cook, M.M. Tentzeris, “Inkjet Printing of Multilayer Millimeter-Wave Yagi-Uda Antennas on Flexible Substrates”, in *IEEE Antennas and Wireless Propagation Letters*, vol.15, no., pp.143-146, 2016.

[98] Y. Li, K. Luk, “60-GHz Dual-Polarized Two-Dimensional Switch-Beam Wideband Antenna Array of Aperture-Coupled Magneto-Electric Dipoles”, in *IEEE Transactions on Antennas and Propagation*, vol.64, no.2, pp.554-563, Feb. 2016.

[99] J. Wu, Y.J. Cheng, Y. Fan, “Millimeter-Wave Wideband High-Efficiency Circularly Polarized Planar Array Antenna”, in *IEEE Transactions on Antennas and Propagation*, vol.64, no.2, pp.535-542, Feb. 2016.

[100] V. Semkin, F. Ferrero, A. Bisognin, J. Ala-Laurinaho, C. Luxey, F. Devillers, A.V. Raisanen, “Beam Switching Conformal Antenna Array for mm-Wave Communications”, in *IEEE Antennas and Wireless Propagation Letters* , vol.15, no., pp.28-31, 2016.

[101] D.J. Bisharat, L. Shaowei, X. Quan, “High Gain and Low Cost Differentially Fed Circularly Polarized Planar Aperture Antenna for Broadband Millimeter-Wave Applications”, in *IEEE Transactions on Antennas and Propagation*, vol.64, no.1, pp.33-42, Jan. 2016.

[102] K. Hashimoto et al., “A post-wall waveguide center-feed parallel a High Resistivity Silicon Wafer for 60 GHz WPAN”, *IEEE Transactions on Antennas and Propagation*, March 2010.

[103] A. Lamminen et al., “High gain 60 GHz LTCC chain antenna array with substrate integrated waveguide feed network”, European Conference on Antennas and Propagation (EuCAP), 2012.

[104] Patterson et al., “60 GHz Active Receiving Switched Beam Antenna Array with integrated Butler Matrix and GaAs Amplifiers”, *IEEE Transactions on Microwave Theory and Techniques*, Nov.2012.

[105] J. Schoebel et al., “Design considerations and technology assessment of phased-array antenna systems with RF MEMS for automotive radar applications”, *IEEE Transactions on Microwave Theory and Techniques*, Vol.53, No. 6, June 2005.

[106] Y. Cheng et al., “Millimeter-wave substrate integrated multibeam antenna”, *IEEE Transactions on Antennas and Propagation*, Sep. 2008.

[107] F. Rusek, et al., “Scaling Up MIMO: Opportunities and challenges with very large array”, in *IEEE Signal Processing Magazine*, January 2013.

[108] R. W. Heath Jr. et al., “An overview of Signal Processing Techniques for Millimiter Wave MIMO Systems”, to appear in *IEEE Journal of Selected Topics in Signal Processing*, April 2016. Available on arXiv: 1512.03007v1.

[109] T.S. Rappaport, R. W. Heath Jr., R. C. Daniels, and J. Murdock, *Millemeter Wave Wireless Communications*. Prentice-Hall, September 2014.

[110] A. Leee Swindlehurst, et atl., “Millimeter-wave Massive MIMO: The next wireless revolution?”, in *IEEE Communications Magazine*, Sept. 2014

[111] S. Hur, et al., “Millimeter Wave Beamforming for Wireless Backhaul and Access in Small Cell Networks”, *IEEE Trans. on Communications*, vol. 61, no. 10, October 2013.

[112] A. M. Sayeed, N. Behdad, “Continuous aperture phased MIMO: Basic theory and applications”, *Proc. 2010 Annual Allerton Conf. on Communications, Control and Computers*, Sept. 2010.

[113] O. El Ayach, et al., “Spatially Sparse Precoding in Millimeter Waver MIMO Systems”, *IEEE Trans. on Wireless Communications*, vol 13, no. 3, March 2014.

[114] X. Yu, J. C. Shen, J. Zhang, K. B. Letaief, “Alternating Minimization Algorithms for Hybrid Precoding in Millimeter Wave MIMO systems”, arXiv: 1601.0734v1, January 2016.

[115] J. Singh, S. Ramarkrishna, “On the Feasibility of Codebook-based Beamforming in Millimeter Wave Systems with Multiple Antenna Arrays”, *IEEE Trans. on Wireless Communications*, vol. 14, no. 5, May 2015.

[116] A. M. Sayeed, N. Behdad, “Hybrid analog-digital phased MIMO transceiver system”, Patent no. US 8,811,511 B2, Aug. 2014.

[117] A. Sayeed, *Millimeter-Wave MIMO Architecures for 5G Gigabit Wireless*, plennary talk al the Intl. Workshop on Emerging Technologies for 5G Wireless Cellular Networks, Globecom 2014. Available at http://wcsp.eng.usf.edu/5g/2014/files/5G_Plenary3_AkbarMSayeed.pdf.

[118] A. Alkhateeb, G. Leus, R. W. Heath Jr., “Limited Feedback Hybrid Precoding for Multi-user Millimeter Wave Systems”, *IEEE Trans. on Wireless Communications*, vol. 14, no. 11, pp. 6481-6494, Nov. 2015.

[119] A. Alkhateeb, R. W. Heath Jr., “Frequency Selective Hybrid Precoding for Limited Feedback Millimeter Wave Systems”, submitted to *IEEE Trans. on Communications* (invited paper), ArXiv:1510.00609v2, April 2016.

[120] J. Singh, O. Dabeer, U. Madhow, “On the limits of communication with low-precision analog-to-digital conversion at the receiver”, *IEEE Trans. on Communications*, vol. 57, no 12, pp. 3629 – 3639, 2009.

[121] = [Heath15]?

[122] J. Mo, R.W. Heath Jr., “Capacity analysis of one-bit quantized MIMO systems with Transmitter Channel State Information”, *IEEE Trans. on Signal Processing*, vol. 63, no. 20, Oct. 2015.

[123] J. Mo, et al., "Hybrid Architectures with few-bit ADC receivers: achievable rates and energy-rate tradeoffs", arXiv:1605.00668v1, May 2016.

[124] Z. Xiao, P. Xia, X. Xia, "Low Complexity hybrid precoding and channel estimation based on hierarchical multi-beam search for millimeter-wave MIMO systems", arXiv:1603.01634v1, Mar 2016.

[125] T.A. Thomas and F.W. Vook, "Method for obtaining full channel state information for RF beamforming", in *Proc. IEEE Global Communications Conference (GLOBECOM)*, Dec. 2014.

[126] C.K. Wen et al., "Joint Channel-and-Data Estimation for Large MIMO Systems with Low-precision ADCs", arXiv: 1501.05580, January 2015.

[127] A. Alkhateeb, G. Leus, R.W. Heath Jr., "Compressed sensing based multi-user millimeter wave systems: How many measurements are needed?", in *Proc. of the IEEE Intl. Conf. on Acoustics, Speech, and Signal Processing (ICASSP)*, April 2015.

[128] Z. Gao, et al., "Channel Estimation for Millimeter-Wave Massive MIMO with Hybrid Precoding over Frequency-Selective Fading Channels", arXiv: 1604.03049v1, April 2016.

[129] R. Taori, and A. Sridharan, "Point-to-multipoint in-band mmWave backhaul for 5G networks", *IEEE communication magazine*, pp 195-201, Jan. 2015.

[130] K. Zheng, L. Zhao, J. Mei, M. Dohler, W. Xiang and Y. Peng, "10 Gb/s HetSNets with Millimeter-Wave Communications: Access and Networking – Challenges and Protocols", *IEEE communication magazine*, pp 222-231, Jan. 2015.

[131] R. Baldemair, T. Irnich, K. Balachandran, E. Dahlman, G. Mildh, Y. Selén, S. Parkvall, M. Meyer and A. Osseiran, "Ultra-dense networks in millimeter-wave frequencies", *IEEE communication magazine*, pp 202-208, Jan. 2015.

[132] D. Astely et al., "LTE Release 12 and Beyond", *IEEE Communication Magazine*, vol. 51, no. 7, pp. 154–60, July 2013.

[133] S. Rangan, T. S. Rappaport, and E. Erkip, "Millimeter-wave cellular wireless networks: Potentials and challenges", Proceedings of the IEEE, vol. 102, no. 3, pp. 366–385, 2014.

[134] C. Jeong, J. Park and H. Yu, "Random Access in Millimeter-Wave Beamforming Cellular Networks: Issues and Approaches", *IEEE Communications Magazine*, Jan. 2015.

[135] T. Bai, A. Alkhateeb, and R. W. Heath, "Coverage and Capacity of Millimeter-Wave Cellular Networks', *IEEE Communication Magazine*, Sept. 2014.

[136] K. Zheng, L. Zhao, J. Mei, M. Dohler, W. Xiang, and Y. Peng, "10 GB/s HetsNets with Millimeter-Wave Communications: Access and Networking – Challenges, Methodology, and Applications", *IEEE Communication Magazine*, Jan. 2015.

[137] R. J. Weiler, W. Keusgen, M. Peter, I. Filippini, V. Sciancalepore, and T. Haustein, *Millimeter-Wave Small-Cell Deployment Scenarios as an Enabler for 5G Applications and Use Cases*, 2015.